Research Square

Preprints are preliminary reports that have not undergone peer review.
They should not be considered conclusive, used to inform clinical practice,
or referenced by the media as validated information.

Long term pulmonary exposure to spherical and fibrous aggregates of carbon nanohorns does not induce lung cancer or pleural mesothelioma in Rats: A two-year study

Omnia Hosny Mohamed Ahmed
Nagoya City University
Aya Naiki-Ito
Nagoya City University
David Bedell Alexander
dalexand@phar.nagoya-cu.ac.jp

Nagoya City University
Dina Mourad Saleh
Assiut University
William Theodore Alexander
Nagoya City University
Hiroshi Takase
Nagoya City University
Satoru Takahashi
Nagoya City University
Akihiko Hirose
Chemicals Evaluation and Research Institute
Ryota Yuge
NEC (Japan)
Masako Yudasaka
Suwa University of Science
Sumio iijima
Meijo University
Hiroyuki Tsuda
Nagoya City University

Research Article

Keywords: Carbon nanotube, Carbon nanohorn, Carbon nanobrush, Intra-tracheal intra-pulmonary spraying

Posted Date: June 11th, 2026

DOI: https://doi.org/10.21203/rs.3.rs-9426445/v1

License: This work is licensed under a Creative Commons Attribution 4.0 International License.
Read Full License

Additional Declarations: No competing interests reported.

Long term pulmonary exposure to spherical and fibrous aggregates of carbon nanohorns does not induce lung cancer or pleural mesothelioma in Rats: A two-year study

Omnia Hosny Mohamed Ahmed [1,2,3*], Aya Naiki-Ito [2*], David B. Alexander [1], Dina Mourad Saleh [4], William T. Alexander [1], Hiroshi Takase [5], Satoru Takahashi [2], Akihiko Hirose [6], Ryota Yuge [7], Masako Yudasaka [8,9], Sumio Iijima [10],and Hiroyuki Tsuda [1*]

[1] Nanotoxicology Lab Project, Nagoya City University, Nagoya, Japan

[2] Department of Experimental Pathology and Tumor Biology, Nagoya City University, Nagoya, Japan

[3] Department of Forensic Medicine and Clinical Toxicology, Aswan University, Aswan, Egypt

[4] Department of Forensic Medicine and Clinical Toxicology, Assuit University, Assuit, Egypt

[5] Core Laboratory, Graduate School of Medical Sciences, Nagoya City University, Nagoya, Japan

[6] Chemicals Evaluation and Research Institute (CERI), Tokyo, Japan

[7] Secure System Platform Research Laboratories, NEC Corporation, 1-1-1 Umezono, Tsukuba, Ibaraki, Japan.

[8] Department of Mechanical and Electrical Engineering, Faculty of Engineering, Suwa University of Science, Chino, Nagano, Japan

[9] Faculty of Science and Technology, Meijo University, Nagoya, Japan

[10] Graduate School of Science and Technology, Meijo University, Nagoya, Japan

*Corresponding author:
Omnia Hosny Mohamed Ahmed: omnia.hosny@aswu.edu.eg
Aya Naiki-Ito: ayaito@med.nagoya-cu.ac.jp
David B. Alexander: dalexand@phar.nagoya-cu.ac.jp
Hiroyuki Tsuda: htsuda@phar.nagoya-cu.ac.jp

Abstract

Background Fibrous carbon nanohorn aggregates have extremely high electrical conductivity. Carbon nanohorns (CNHs), like single-walled carbon nanotubes (SWCNTs), are composed of single graphene cylinders. However, in contrast to SWCNT in which the graphene cylinder is open ended and can be of different lengths, CNHs are composed of graphene cylinders which are closed at one end and have lengths of approximately 40-50 nanometers. CNHs can assemble radially to form spherical CNH aggregates or assemble into fibrous aggregates known as a carbon nanobrushes. We have previously investigated the toxicity and carcinogenicity of several different MWCNTs administered to the rat lung by intra-Tracheal

Intra-Pulmonary Spraying (TIPS). In the present study we used TIPS to investigate the pulmonary and pleural toxicity of spherical and fibrous CNH aggregates in the rat. **Results:** Spherical and fibrous CNH aggregates (0.5 and 1 mg/rat) were administered into the rat lung, using MWCNT-7 (0.5 mg/rat) as the reference material. After administration of CNH aggregates into the rat lung, CNHs were biopersistent in the lung for 2 years. However, they didn't induce pulmonary inflammation or fibrosis. In contrast, MWCNT-7 induced marked pulmonary and pleural inflammation and fibrosis. No Lung Carcinomas or Mesotheliomas developed in the rats administered spherical of fibrous CNH aggregates. One rat in the 1 mg spherical CNH aggregate group developed a bronchiolo-alveolar adenoma (1/12), however, this was not statistically significant compared to the vehicle controls (0/11). All of the rats administered MWCNT-7 developed Visceral (6/13) and/or Pleural Mesothelioma (13/13). **Conclusion:** This is the first 2-year study to assess the carcinogenicity of CNH aggregates. Our results demonstrate that neither spherical nor fibrous aggregates of CNH are carcinogenic to the rat lung or pleura.

Key Words

Carbon nanotube, Carbon nanohorn, Carbon nanobrush, Intra-tracheal intra-pulmonary spraying

Background

The synthesis of carbon nanotubes (CNTs) was first reported by Iijima in 1991 [1]. CNTs are composed of coaxial tubes of graphene sheets, and CNTs that differ in the number of constituent coaxial tubes (commonly referred to as constituent walls), length, and physico-chemical properties can be manufactured. The wide variety of manufactured CNTs coupled with their remarkable mechanical, thermal, chemical, and electrical properties, make CNTs extremely valuable with numerous industrial and biomedical applications: for example, see the Introduction of Gupta et al. [2]. One of the properties of CNTs is that they are very light in weight. However, this makes them easily airborne and inhaled. Consequently, there are concerns about their effects on human health.

Initial carcinogenicity studies used intrascrotal and intraperitoneal injection to investigate the carcinogenic potential of CNTs [3, 4, 5, 6, 7, 8]. These studies found that thick rigid CNTs were carcinogenic but that thin flexible CNTs were not carcinogenic. Sargent et al. reported that exposure to multiwalled carbon nanotube-7 (MWCNT-7, also known as Mitsui 7), a thick rigid CNT, by inhalation promoted

methylcholanthrene-initiated lung adenocarcinoma growth and progression [9], and in 2014 the International Agency for Research on Cancer (IARC) determined that there was sufficient evidence to conclude that MWCNT-7 was carcinogenic in experimental animals and possibly carcinogenic in humans and classified MWCNT-7 as a Group 2B (Possibly carcinogenic to humans) agent [10, 11]. However, IARC concluded that there was insufficient evidence available to classify the carcinogenicity to humans of any other CNT, and therefore classified all other CNTs as Group 3 (Not classifiable as to its carcinogenicity to humans) agents [10, 11].

The fibre pathogenicity paradigm predicts that longer rigid fibers are potential carcinogens when inhaled into the lung [12, 13]. The fibre pathogenicity paradigm concludes that carcinogenic potential is based primarily on retention of fibers in the lungs and pleural cavity coupled with induction of inflammation and predicts that thin flexible CNTs will have little carcinogenic potential when inhaled. This agrees with the results of the intrascrotal and intraperitoneal injection studies. However, as described by Nagai et al. and by Ahmed et al., the reason why intrascrotal and intraperitoneal injection of thin flexible CNTs was not carcinogenic is because they do not damage mesothelial cells [5, 14]. In agreement with the fiber pathogenicity paradigm, thick rigid CNTs do damage mesothelial cells and retention of these CNTs in the pleural/peritoneal cavity results in chronic tissue damage and inflammation resulting in the development of mesothelioma.

Long term carcinogenicity studies (the assessment of whether a substance can cause cancer following prolonged or lifetime exposure) of MWCNTs published prior to 2025 are reviewed by Ahmed et al. [14]. Long term studies have demonstrated that whole body inhalation exposure to MWNCT-7 and intratracheal instillation of MWCNT-7 resulted in the development of lung cancer and pleural mesothelioma in rats [15, 16, 17]; intratracheal instillation of MWCNT-N, a rigid CNT similar to MWCNT-7, resulted in the development of lung cancer and pleural mesothelioma in rats [18]; and intratracheal instillation of the thin flexible CNTs, MWCNT-B and double-walled CNT (DWCNT) resulted in the development of lung cancer in rats [19, 20, 21]. Therefore, both thick rigid CNTs and thin flexible CNTs are potential human carcinogens when inhaled, with thick rigid CNTs causing both lung cancer and pleural mesothelioma and thin flexible CNTs causing lung cancer in experimental animals.

In 1993 two groups, Iijima and Ichihashi and Bethune et al., reported the generation of single-walled carbon nanotubes (SWCNT) [22, 23]. An initial study by Honda et al., 2017, reported that administration of short SWCNT by a single intratracheal instillation resulted in chronic inflammation and a single intratracheal

instillation of long SWCNTs resulted in fibrosis in rats [24]. In their study, SWCNTs were not genotoxic and did not induce the development of lung tumors or pleural mesothelioma, however, the development of fibrosis and chronic inflammation supports the possibility that inhalation of SWCNTs is toxic to humans. In a more recent study, Naiki-Ito et al. report that administration of SWCNTs by intratracheal instillation twice a week for 4 weeks did result in the development of lung cancer in rats (Naiki-Ito et al., unpublished observations).

In 1999 Iijima reported the generation of a new type of carbon nanotubular material, single-walled graphitic carbon nano-horns, that coalesce into spherical aggregates [25], also see Harris et al. (1994) and Harris (2005) [26, 27]: in the present report these single-walled graphitic carbon nano-horns are referred to single-walled carbon nanohorns (SWCNHs) and the spherical aggregates are referred to as spherical-SWCNHs (sph-SWCNHs). SWCNHs are composed of single graphene cylinders, closed at one end with lengths of 40-50 nanometers. In the spherical aggregates formed by SWCNHs, individual SWCNHs coalesce at the aggregation center forming stable spherical structures [25, 28]. In 2009 individual SWCNHs were isolated from these aggregates and characterized by Zhang et al. [29]. A second type of SWCNH aggregate was described by Yuge et al. [30, 31]. In the second type of aggregate, individual SWCNHs aggregate along a central CNT, likely a SWCNT or a bundle of SWCNTs, and the SWCNHs and the central CNT structure coalesce at high temperatures to form stable fibrous aggregates. These fibrous aggregates, initially referred to as fib-CNHs [30], have a shape similar to a bottle cleaning brush, so they are also referred to as carbon nano-brushes (CNBs) [31].

Both sph-SWCNHs and CNBs can be prepared using a conventional SWCNH manufacturing system, enabling their production on a large scale [30]. The high dispersibility and large surface area of sph-SWCNHs making them very attractive materials for energy devices like supercapacitors and fuel cells, for applications in gas adsorption and storage, and for nanomedicine such as drug delivery and photo-hyperthermia cancer therapy [32]. Also, the unique fibrous structure of CNBs enhances their electrical conductivity and dispersibility in solution. These outstanding characters makes them promising candidate for the electrode material in devices such as supercapacitors, electrochemical actuators, fuel cells, lithium-ion batteries, and sensing devices [33].

As noted above, SWCNHs, like SWCNTs, are composed of single graphene cylinders. However, the graphene tubules composing SWCNHs are closed at one end and the lengths, approximately 40-50 nanometers [25, 28], are shorter than those of the majority of SWCNTs (see Streit et al. 2012 [34]). Thus, the composition

of SWCNHs and SWCNTs are the same but the structures differ. Consequently, the toxicity of SWCNTs and SWCNHs may also differ.

Initial toxicology studies of SWCNHs were carried out by Miyawaki et al. [35]. Using spherical aggregates of SWCNHs, they carried out skin and eye irritation tests, skin sensitization tests, peroral administration, intratracheal instillation, reverse mutation tests, and chromosomal aberration tests using rabbits, guinea pigs, and rats. They reported that sph-SWCNHs exhibited little or no acute or subchronic toxicity. However, long-term toxicity studies were not performed.

In the present study, sph-SWCNHs and CNBs were administered to rats via intratracheal intrapulmonary spraying (TIPS) once every other day over the course of 2 weeks for a total of 8 administrations. A total of 0.5 and 1 mg of sph-SWCNHs and CNBs were administered and the experimental rats were then observed for 2 years. In contrast to the studies investigating the toxicity of CNTs cited above, in the present study intratracheal instillation of sph-SWCNHs and CNBs did not induce chronic inflammation, fibrosis, or lung or pleural cancer. Our long-term study together with the acute and subchronic toxicity studies by Miyawaki et al. [35], indicate that current experimental evidence supports the premise that SWCNHs are not toxic/carcinogenic in experimental animals.

Materials and Methods

Nanomaterials

Three types of nanomaterials were used in the present study: spherical aggregates of Carbon NanoHorns (sph-SWCNHs); fibrous aggregates of Carbon NanoHorns, referred to as Carbon Nano-Brushes (CNBs) in the present study; and MWCNT-7. sph-SWCNHs and CNBs were supplied by NEC Corporation (Kawasaki, Japan). sph-SWCNHs were prepared at room temperature by the CO_2 laser ablation of carbon without metal catalyst [25]. CNBs were prepared by CO_2 laser ablation of a carbon target with an iron content of 1% at room temperature [30]. MWCNT-7 was provided by Mitsui Chemicals Inc., (Tokyo, Japan) with an iron content of 0.3% by weight.

Preparation of sph-SWCNHs, CNBs, and MWCNT-7

The nanomaterials were weighed and dispersed in tert-butyl alcohol by sonication for 10 min and stored frozen at −20 °C. Shortly before administration, the T-butyl alcohol was removed using an Eyela Freeze Drying

machine (FDU-2110; Tokyo Rikakikai Co., Ltd., Tokyo, Japan), and the sph-SWCNH, CNB, and MWCNT-7 were suspended in saline containing 0.5% Pluronic F-68 (PF68, Sigma-Aldrich, St. Louis, MO, USA) at concentrations of 62.5 and 125 μg/ml (sph-SWCNH and CNB) and 125 μg/ml (MWCNT-7). The suspension was sonicated for 2 min four times at 3000 rpm using a polytron PT 1600E bench top homogenizer (Kinematika AG, Lattau, Switzerland). Immediately prior to administration, the suspensions were sonicated for 30 min using a water bath sonicator for sph-SWCNH and CNB, and a Tomy Ultrasonic disruptor, UD-211, equipped with a TP-040 micro tip (Tomy Seiko Co., Ltd., Tokyo, Japan) at a power setting of 4 for MWCNT-7. After sonication and before TIPS administration, samples of the test materials were collected for examination by TEM and SEM.

Animals

Ten-week-old male F344 (F344/DuCrlCrlj) rats were purchased from Charles River Laboratories Japan Inc., Yokohama, Japan. The animals were housed in the Animal Facility of the Graduate School of Medical Sciences, Nagoya City university, maintained on a 12 h light–dark cycle, and received Oriental MF basal diet (Oriental Yeast Co., Tokyo, Japan) and tap water ad libitum. The research protocol was approved by the Animal Care and Use Committee of Nagoya City University Medical School (approval number H27-P-5), and the research was conducted according to the Guidelines for the Care and Use of Laboratory Animals of Nagoya City University. The experiment was started after a 2-week acclimation and quarantine period.

Experimental design

After acclimatization for 2 weeks, a total of 142 rats 12 weeks old were divided into six body weight matched groups: Group 1 (20 rats), without treatment; Group 2 (20 rats), vehicle administered (saline with 0.5% Pluronic F-68); Group 3 (20 rats), administered 0.5 mg sph-SWCNH per rat; Group 4 (20 rats), administered 1 mg sph-SWCNH per rat; Group 5 (20 rats), administered 0.5 mg CNB per rat; Group 6 (20 rats), administered 1 mg CNB per rat; and Group 7 (22 rats), administered 1 mg MWCNT-7 per rat. Rats were administered the test solutions by TIPS. Briefly, rats were anesthetized with 3% isoflurane and administered 0.5 ml vehicle or test material suspensions (62.5 μg or 125 μg of test material in 0.5 ml vehicle) using a micro sprayer (series IA–1B Intratracheal Aerosolizer Penn-century, Philadelphia, PA). Rats were administered one dose every other day over a 14-day period: 8 administrations for total doses of 0.5 mg or 1 mg sph-SWCNH and CNB per

rat and 1 mg MWCNT-7 per rat. The rats were examined weekly for body weight measurement and signs of toxicity until week 6 (4 weeks after the final TIPS administration). From week 6 until the final sacrifice the rats were observed once a month. At week 6 (4 weeks after the final TIPS administration), five rats from each group were sacrificed and the remaining rats were kept without further treatment until the final sacrifice. Twelve rats died before week 55 from causes unrelated to the treatment and were excluded from the study. Carcinogenic lesions in the lungs and pleura were evaluated in all animals that lived for 55 weeks or longer. In the MWCNT-7 group, seven animals died due to development of malignant pleural mesothelioma before week 75, with the earliest death occurring at week 55. Due to animal welfare considerations, the remaining 10 animals in this group were sacrificed at week 75. The final sacrifice of the untreated, vehicle, sph-SWCNHs, and CNBs treated rats was performed at week 104. Throughout this report, the final sacrifice refers to the terminal sacrifices performed at week 75 for MWCNT-7 treated rats and week 104 for the other groups.

Characterization of the test materials before and after TIPS administration

After sonication, described above, and immediately before administration to the rats' lungs, 20 µl of each test material suspension was placed on a microgrid membrane attached to a copper mesh (EMS 200-Cu, Nisshin EM Co., Ltd., Tokyo, Japan) for measurement of sph-SWCNHs, CNBs, and MWCNT-7 fibers prior to TIPS administration. The shape of the nanoparticles was imaged by SEM (Field Emission Scanning Electronic Microscope; Hitachi High Technologies, Tokyo, Japan) and TEM (Transmission electron microscope; EDAX, Tokyo, Japan) and the photos were analyzed by NIH image analyzer software (NIH, Bethesda, MD, USA).

For Characterization of sph-SWCNHs and CNBs in the lungs of rats at 104 weeks after instillation about 1 gm of paraformaldehyde fixed lung tissue was digested as previously described [36]. Briefly, tissues were incubated in Clean 99-K200® (Clean chemical Co., Ltd., Ibaraki, Japan) overnight or until complete dissolution of lung tissues. The digested solution was then centrifuged at 12,000 rpm for 30 min and the supernatant was discarded. The pellet was resuspended in distilled water and sonicated by a short burst (approximately 2–3 s) from a micro-ultrasonic cell disruptor (Misonix Incorporated). The resuspended CNH aggregates were collected by centrifugation and washed two more times, then resuspended in 200 µl of distilled water and the specimens were collected on EMD Millipore TM Polycarbonate Membrane Filters (Millipore, Tokyo, Japan). Fibers were viewed by SEM (Field Emission Scanning Electronic Microscope; Hitachi High

Technologies, Tokyo, Japan) at 5–10 kV and TEM (Transmission electron microscope; EDAX, Tokyo, Japan) at 15–50 kV.

Tissue sample collection and Histopathological Examination

At necropsy, blood samples were collected via the abdominal aorta under deep isoflurane anesthesia, centrifuged at 3000×g, 4 °C for 10 min, and the serum was collected and stored at −80 °C. Organs, including lung, liver, kidney, spleen, brain, heart, and testes were examined for any macroscopic lesions. The trachea, esophagus, lymph nodes (including mediastinal lymph nodes), diaphragm including the diaphragmatic region of the parietal pleura were examined macroscopically and then processed for histopathological examination.

The 4 right lobes of the lung of each rat were excised at necropsy, frozen in liquid nitrogen, and sored at −80 degrees for further biochemical analysis. The left lung was inflated and fixed with 4% paraformaldehyde solution in phosphate-buffered saline (PBS) adjusted to pH 7.3 and processed for hematoxylin–eosin (H&E) staining and immunohistochemical examination.

Pathological examination and Immunohistochemistry

3 μm-thick sections were prepared from the fixed, paraffin-embedded specimens and stained with Hematoxylin and Eosin (H&E). Underlying sections were immunohistochemically stained with antibodies to CD68 (BMA Biomedicals, Augst, Switzerland) and PCNA (Abcam, Cambridge, UK). H&E-stained tissue sections were evaluated by two board-certified Pathologists of the Japanese society of Toxicologic pathology, Drs. Hiroyuki Tsuda and Satoru Takahashi, and diagnosis of hyperplasia, adenoma, adenocarcinoma, and mesothelioma was done according to the INHAND criteria. The total counts of granulomas, the total counts of CD86 positive macrophages, and the PCNA index were carried out as previously described [19].

Collagen deposition in lung tissues and the visceral and partial pleura was quantified using light microscopic images of lung tissues and pleural sections stained with Masson's Trichrome (Abcam, Tokyo, Japan) using NIH image analyzer software (NIH, Besthesda, Meryland, USA): ten individual images were captured from 2 lung and 3 diaphragm sections from 3 rats per study group. Thresholding using pre-defined RGB criteria for collagen deposition was performed. This allowed collagen to be differentiated from alveolar tissue or pleural tissue. The surface area of fibrosed tissue was measured. Total lung alveolar and pleural tissue

surface areas were measured using an image analyzer (KEYENCE BZ-X810). The results are expressed as the percentage area of pulmonary/pleural collagen deposition per unit of tissue surface area.

Electron microscopic viewing of fibers in lung tissues

For high magnification viewing, H&E-stained slides were immersed in xylene for 2–3 days to remove the cover glass, immersed in 100% ethanol for 10 min to remove the xylene, and air-dried for 2 h at room temperature. The slides were then coated with a layer of sublimated OsO4 using an osmium plasma coater (OPC80N; Filgen, Nagoya, Japan) for viewing by SEM (S-4800, Hitachi High Technologies, Tokyo, Japan). For ultrafine viewing, a small piece of paraformaldehyde fixed lung tissue was imbedded in epoxy resin and processed for TEM (EDAX, Tokyo, Japan).

RNA extraction, cDNA synthesis, and quantitative reverse transcription–PCR analysis of gene expression

Total RNA was isolated from frozen lung tissues by phenol–chloroform extraction (Isogen; Nippon Gene Co. Ltd., Tokyo, Japan). One microgram of RNA was converted to cDNA using Prime Script™ RT Master Mix (Takara). The cDNA was subjected to quantitative real-time PCR (qRT-PCR) using TB Green™ Premix Ex Taq™ II (Takara) and detected by the Aria Mx Real-Time PCR System (g8830a, RRID:SCR_019469, Agilent Technologies). β-actin was used as the endogenous reference housekeeping gene. Target genes were normalized to β-actin. Primers were designed using NCBI software (https://www.ncbi.nlm.nih.gov) and purchased from Sigma-Aldrich. Primers are listed in Additional file 1. Data are expressed as mean ± standard deviation (SD) and statistical significance between groups was analyzed using one- way analysis of variance (ANOVA). Multiple comparisons were analysed using the Tukey-HSD method. P-values < 0.05 were considered to be significant.

Detection of ROS production

Six μm thick slices were cut from the frozen lung tissues of rats sacrificed at 6 weeks (4 weeks after the final TIPS administration) and incubated in 5 μM Dihydroethidium (DHE, a specific fluorescent dye for $O_2^{\cdot-}$, Thermo Fisher Scientific) for 15 min in the dark. The slides were washed with phosphate buffered saline and ROS was detected at 518/605 nm using an image analyzer (BZ 9000 Fluorescence Microscope,

RRID:SCR_015486, Keyence, Osaka, Japan). Ten images per rat were randomly taken with the same exposure time at 400 × magnification, and the average fluorescence intensity in the alveolar epithelial nuclei was quantified using BZ-analysis application software (Keyence).

Statistical analysis

Survival curves were plotted according to the method of Kaplan-Meier. The incidences of neoplastic lesions in the lung and pleura were analyzed for significant difference from vehicle treated control by Fisher's exact test. Quantitative data were expressed as mean ± standard deviation (SD) and Statistical significance between groups was analyzed using a 2-sided t-test using the GraphPad Quick calculator. P-values < 0.05 were considered to be significant.

Results

Characterization of test materials

Figure 1 illustrates single-walled carbon nanohorns (SWCNHs) and its aggregates, spherical carbon nanohorns (sph-SWCNHs) and brush like aggregates (CNBs). Figure 2 shows representative TEM and SEM photos of sph-SWCNHs, CNBs, and MWCNT-7 fibers in suspension prior to TIPS administration. Fiber lengths and diameters are presented in Table 1. sph-SWCNHs are formed from spherical aggregation of SWCNHs [25]. Figure 2a shows the sph-SWCNHs used in the present study consisted of multiple nearly uniform sized spherical particles 72 ± 17 nm in diameter, and Figure 2d shows that these sph-SWCNHs grouped together to form large agglomerate structures. CNBs are formed from fibrous aggregation of SWCNHs [30, 31]. Figure 2b shows the linear structure of CNBs and Figure 2e shows that the CNBs used in the present study retained their individual structure and did not assemble into larger agglomerates. MWCNT-7 fibers are relatively thick, straight, individual fibers with diameters of 76.49 ± 31.14 nm (Figure 2c) and lengths of 8.79 ± 4.41 μm (Figure 2f).

Figure 1 Single-walled carbon nanohorns (SWCNHs) and its aggregates.

(a) SWCNHs are formed from single graphene tubules. The tubules are closed at one end and are approximately 40-50 nm in length. (b,c) SWCNHs form stable spherical aggregates (sph-SWCNH) [25]. (d,e) In a second type of aggregate, individual SWCNHs aggregate along a central CNT forming fibrous, brush

like aggregates (CNB) [31]. The illustrations shown in (a), (b), and (d) and the TEM image shown in (c) are taken from © NEC Corporation 1994-2026 (https://jpn.nec.com/rd/pht/carbonnanotube.html and https://s3-service-broker-live-19ea8b98-4d41-4cb4-be4c-d68f4963b7dd.s3.amazonaws.com/uploads/ckeditor/attachments/8277/Advertisement_NEC_Corporation.pdf) with permission from NEC Co. The TEM image of the CNB shown in (e) is re-used from "Preparation and Characterization of Newly Discovered Fibrous Aggregates of Single-Walled Carbon Nanohorns", Yuge et al., DOI: 10.1002/adma.201602022 with the permission of John Wiley and Sons.

Figure 2 Transmission (TEM) and scanning electron microscopic (SEM) characterization of aggregates in the vehicle before administration.

(**A**) TEM images. (a) sph-SWCNH: single-walled carbon nanohorn tubules forming spherical aggregates. (b) CNB: fibrous aggregation of SWCNHs forming a shape similar to a bottle cleaning brush, (c) MWCNT-7: thick rigid fibers.

(**B**) SEM images. (d) An agglomerate composed of numerous sph-SWCNHs, (e) CNB, fiber-shaped agglomerate of SWCNHs, (f) MWCNT-7 fibers form fibrous structures of variable length and thickness. The average lengths of the particles are indicated the figure.

Table 1 Characterization of sph-SWCNH, CNB, and MWCNT-7 individual particles and agglomerates suspended in the vehicle.

	Individual particles		
	sph-SWCNH	CNB	MWCNT-7
Length	72 ±17nm	1.4±1.1μm	8.8±4.4μm
Diameter	72 ±17nm	58±18nm	76±31nm
Iron content (wt%)	0[a]	1[b]	0.3[c]
	Agglomerates		
Length	0.9±0.3 μm[d]	1.4±1.1μm	8.8±4.4μm

[a] Iigima et al.,1999 [25].

[b] Yuge et al., 2016 [30]

[c] Sakamoto et al., 2009 [6]

[d] Individual sph-SWCNH aggregates are grouped together forming a large agglomerate structure.

Interim sacrifice

Rats were divided into seven groups: no treatment (20 rats); rats administered vehicle alone (20 rats); rats administered 0.5 mg sph-SWCNHs (20 rats); rats administered 1 mg sph-SWCNHs (20 rats); rats administered 0.5 mg CNBs (20 rats); rats administered 1 mg CNBs (20 rats); and rats administered 1 mg MWCNT-7 (22 rats). At week 6 (4 weeks after the final TIPS administration) an interim sacrifice was performed on 5 rats from each group. No clinical symptoms of toxicity were found in any of the treated groups. The lungs and mediastinal lymph nodes of the treated rats had gray to black colored sph-SWCNH/CNB/MWCNT-7 depositions. The colored areas of the lungs tended to be larger in the sph-SWCNH groups than in the CNB groups. The parabronchial and mediastinal lymph nodes of the sph-SWCNH and CNB treated rats were dark gray, and the parabronchial and mediastinal lymph nodes of the MWCNT-7 treated rats were entirely black. No macroscopic lesions were found.

Observation of the fibers in the lung tissue at week 6

At week 6, sph-SWCNHs and CNBs, by light microscope, appeared as dense black material completely engulfed by groups of alveolar macrophages in the alveolar space and had a homogenous dark color under polarized light (Figure 3a,b). In contrast, MWCNT-7 appeared as finely granular to elongated black fibers, with some fibers protruding from the alveolar macrophage cell membrane, and had bright whitish color under polarized light (Figure 3c). Notably, some free MWCNT-7 fibers were also found in the alveolar space. SEM images show that sph-SWCNHs and CNB fibers formed a regular compact mass inside the cytoplasm of alveolar macrophages (Figure 3d,e), while MWCNT-7 fibers are long and needle shaped and penetrate the alveolar macrophage cell membrane (Figure 3f).

Figure 3 sph-SWCNH, CNB, and MWCNT-7 in the lung alveoli at week 6.

(**A**) H&E images. (a) and (b) sph-SWCNH and CNB localize in the macrophages and do not cause polarization (blue framed arrows). (c) As shown in the inset picture, MWCNT-7 is not cleared from the alveolar space. Both free fibers and fibers engulfed by macrophage are found (red framed arrows).

(**B**) SEM images. (d) and (e) sph-SWCNH and CNB are clearly internalized by alveolar macrophages. (f) MWCNT-7 fibers are incompletely internalized by alveolar macrophages and numerous fibers extending into the alveolar space can be seen.

Histopathological evaluation at week 6

Figure 4 shows the early histopathological findings in the lung tissue of the vehicle, sph-SWCNH, CNB, and MWCNT-7 treated groups. Table 2 shows the inflammatory and proliferative parameters in the lung and pleura at week 6. The granuloma count was significantly increased in the sph-SWCNH, CNB, and MWCNT-7 treated groups compared to the vehicle group, and the granuloma count was significantly increased in the MWCNT-7 group compared to the 0.5 mg and 1 mg sph-SWCNH and CNB groups. CD68 immuno-histochemistry showed significantly increased numbers of alveolar macrophages in the alveolar space in the sph-SWCNH, CNB, and MWCNT-7 treated groups compared with the vehicle group. Treatment with sph-SWCNH and CNB did not increased the PCNA labelling index of either alveolar epithelial or pleural mesothelial cells. In contrast, the PCNA labelling indices of the lung and pleura in the rats administered MWCNT-7 were significantly increased compared to the vehicle group and the sph-SWCNH and CNB groups.

Figure 4 Granuloma formation, CD68 positive macrophages, and alveolar epithelial cell proliferation at week 6.

(A) H.E staining. Lung granulomas in the alveolar space enclosing (b) sph-SWCNH, (c) CNB, (d) and MWCNT-7. Both sph-SWCNH (b) and CNB (c) are better internalized than MWCNT-7 (d).

(B) CD68 (macrophage). Most of the macrophages containing (b) sph-SWCNH, (c) CNB, and (d) MWCNT-7 in the cytoplasm are positive for CD68.

(C) PCNA. In the MWCNT-7 treated lungs (d), but not in the sph-SWCNH (b) or CNB (c) treated lungs, alveolar epithelial cells positive for PCNA is significantly elevated.

Table 2 Cell proliferation and inflammation related parameters in the lung tissue at week 6.

Lesions	Untreated	Vehicle	sph-SWCNH		CNB		MWCNT-7 1 mg/rat
			0.5 mg/rat	1 mg/rat	0.5 mg/rat	1 mg/rat	
Granuloma count/cm^2	0±0	1.2±1.3	39.0±10.6***	112.4±22.1***	29.0±10.1***	112.8±24.3***	259.2±55.2$^{***,\#\#\#,\$\$\$}$
Free Macrophage count/cm^2	106.4±16.3	122.6±14.7	438.6±46.9*	516.4±55.9**	388.8±52.5*	473.0±71.0**	557.4±64.5 $^{***,\#\#\#,\$\$\$}$
Alveolar epithelial cell PCNA index %	6.7±3.3	8.5±3.1	7.5±3.7	9.5±3.7	9.9±2.0	9.8±4.5	14.6±4.2*

Pleural mesothelial cell PCNA index %	6.4±1.8	6.2±3.6	7.7±2.8	8.3±2.5	7.7±1.6	8.5±1.5	17.8±4.2 $^{**,\#\#\#,\$\$}$

Data are presented as mean ± S.D.

5 rats per group were examined.

*,**,*** $p < 0.05, 0.01, 0.001$ vs Vehicle respectively.

$^{\#\#\#}$ $p < 0.001$ MWCNT-7 vs sph-SWCNH 1 mg/rat.

$^{\$\$,\$\$\$}$ $p < 0.01, 0.001$ MWCNT-7 vs CNB 1 mg/rat respectively.

Pro-inflammatory cytokine gene expression in the lung tissue at week 6

Figure 5 and Additional file 2 show pro-inflammatory cytokine gene expression in the lung tissue of rats administered sph-SWCNH, CNB, and MWCNT-7 at week 6. The mRNA expression of Ccl2, Ccl3, and TNF-α was significantly up-regulated in MWCNT-7 treated rats but not in the lungs of the sph-SWCNH and CNB treated rats, compared to the vehicle. The mRNA expression of Cxcl1, Cxcl2, Cxcl3, IL-1 α, and IL-1β were not significantly changed by administration of sph-SWCNH, CNB, or MWCNT-7 compared to the vehicle (Additional file 2).

Figure 5 Ccl2, Ccl3, and TNF-α gene expression at week 6.

Ccl2, Ccl3, and TNF-α gene expression in the lung of rats at week 6 by quantitative RT-PCR in the groups administered 1 mg/rat. All data were standardized using the housekeeping gene β-actin. Each bar represents the mean ± SD. Number of samples= 3 rats/group. **,*** P < 0.01, 0.001, Significantly increased compared to vehicle.

Intracellular ROS generation in the lung tissue at week 6

To investigate the ability of sph-SWCNHs and CNBs to generate ROS in the lung, we analyzed the lung tissue of the rats at week 6 by intracellular staining for O_2^-. DHE (a specific fluorescent dye for O_2^-), was used to monitor ROS generation. In the sph-SWCNH and CNB treated lungs, the fluorescence for O_2^- showed no difference compared to the control groups (Figure 6 and Additional file 3). In contrast, in the MWCNT-7 treated lungs, there was a significant increase in O_2^- fluorescence compared to the control group. O_2^- fluorescence was also significantly greater in the MWCNT-7 treated lungs compared with the sph-SWCNH and CNB treated lungs.

Figure 6 Intracellular reactive oxygen species at week 6.

(A) ROS in the lungs of (a) vehicle, (b,c) sph-SWCNH, (d,e) CNB, and (f) MWCNT-7 treated rats. Red color indicates intracellular localization of O_2^-.

(B) The bar chart showing the signal intensity of fluorescence in each group. Only MWCNT-7, which showed the highest intensity of fluorescence, was significantly different from the control group.

**Significantly increased compared to vehicle control

Survival

One rat from the untreated group; 1 rat from the vehicle group; 5 rats from the 0.5 mg sph-SWCNH group; 2 rats from the 1 mg sph-SWCNH group; 1 rat from the 0.5 mg CNB group; and 2 rats from the 1 mg CNB group were found dead before week 55 (see Additional file 4). These early deaths were unrelated to the treatment, and the early deaths in the sph-SWCNH and CNB groups were not significantly different from the control groups. These rats were excluded from the study. The average survival of the remaining rats is shown in Table **3** and their survival rate is shown in the Kaplan Meier curve in Additional file 5. No significant differences in the average survival period were observed between the untreated group (103w), the vehicle group (101w), the 0.5 mg sph-SWCNH group (102w), the 1 mg sph-SWCNH group (102w), the 0.5 mg CNB group (103w), and the 1 mg CNB group (101w). Neither treatment related deaths nor clinical signs were observed in any sph-SWCNH or CNB administered rats. In the MWCNT-7 administered group, one rat died from pleural mesothelioma at week 55. This rat was not excluded from the study. In this group, 6 more rats died from malignant mesothelioma before week 75. The final sacrifice was performed on the remaining 10 rats in the MWCNT-7 group at week 75.

Table 3 The average survival weeks and survival rate at the final sacrifice.

	Untreated	Vehicle	sph-SWCNH		CNB	
			0.5 mg/rat	1 mg/rat	0.5 mg/rat	1 mg/rat
No. of rats examined [a]	14	14	10	13	14	13

Survival rate %	86	79	80	92	93	77
Average survival time (weeks)	103	101	102	102	103	101

[a] Lived 55 weeks or longer: the first pleural mesothelioma was found in the MWCNT-7 group at week 55.

Observation of the test material in the lung tissue at the final sacrifice

At the final sacrifice, almost all SWCNHs and SWCNH-aggregates in the lung tissue were enclosed by groups of alveolar macrophages forming granulation tissue with very little material found engulfed by free alveolar macrophages. In contrast, at the final sacrifice, relatively high numbers of MWCNT-7 fibers were observed in both granulation tissue and inside free alveolar macrophages. TEM observation showed that aggregates of sph-SWCNHs maintained their shapes and were dispersed as spherical aggregates in the macrophage cytoplasm. In contrast, in rats treated with CNBs, no intact CNB fibers were found in the lungs of these rats. However, the alveolar macrophages in the lungs of these rats did contain sph-SWCNH aggregates (Figure 8): the sph-SWCNH aggregates observed in these macrophages were most likely due to the fact that when CNBs are produced both sph-SWNCHs (sph-CHNs) and CNBs (fib-CNHs) are formed (Yuge et al. [30], also see Fig. 2b and Fig. 2e). The aggregates in TEM images taken after dissolving the lung tissue were the same as in the TEM images taken of intact slide sections from the lung (Figure 8).

Figure 7 Final sacrifice: TEM images of alveolar macrophages of rats administered sph-SWCNH, CNB, and MWCNT-7.

(A) sph-SWCNH aggregates are dispersed in the cytoplasm of macrophages. (B) No CNB aggregates are observed in the macrophage cytoplasm, indicting disaggregation of the CNBs. Due to the simultaneous formation of both CNB aggregates and sph-SWCNH aggregates during assembly of CNB aggregates, sph-SWCNH aggregates are present in the cytoplasm of these macrophages. (C) MWCNT-7 are present as needle-shaped fibers in the cytoplasm of alveolar macrophages. Insets show enlarged views, arrow indicates an MWCNT-7 fiber.

Figure 8 Final sacrifice: TEM images of SWCNH aggregates after digestion of the lung tissue.

At the final sacrifice, in order to observe the SWCNT aggregates in more detail, the lung tissue of the rats administered sph-SWCNH and CNB was digested and the SWCNT aggregates were observed by TEM. There

are no obvious changes in the configuration/shape of sph-SWCNH aggregates. No CNB aggregates are observed, indicting disaggregation of the CNBs. However, due to the simultaneous formation of CNB aggregates and sph-SWCNH aggregates during assembly of CNB aggregates, sph-SWCNH aggregates are present in the lung tissue of CNB treated rats.

Incidence of proliferative lesions at the final sacrifice

Tables 4, 5, and 6 show the incidences of proliferative lesions in the lung, pleura, and other organs at the final sacrifice. No proliferative lesions (in the lung and pleura) were found in any of the rats in the untreated, vehicle, 0.5 mg sph-SWCNH, 0.5 mg CNB, or 1 mg CNB groups. In the 1 mg sph-SWCNH group, one rat developed a bronchioloalveolar adenoma, however, this was not statistically significant compared to the vehicle control group. In the MWCNT-7 group, 13 rats developed parietal malignant pleural mesotheliomas and 6 of these rats also developed visceral pleural mesotheliomas. The incidence of malignant pleural mesothelioma was significantly higher in the rats administered MWCNT-7 (13/17) ($p<0.001$) compared to the vehicle group (0/14). Due to the invasiveness of malignant mesothelioma into the lung tissues, these rats were not assessed for the occurrence of lung lesions. The remaining 4 rats were examined for lung lesions, one rat developed bronchioloalveolar hyperplasia and one rat developed bronchioloalveolar carcinoma. The incidence of combined lesions in the lungs of the rats administered MWCNT-7 (2/4) was statistically significant compared to the vehicle group (0/14). Several of the rats in the sph-SWCNH and CNB treated groups developed other tumors, especially Leydig cell tumors (Table 6). However, none of the tumors was significantly increased in any of the treated groups compared to the control groups, and were consequently concluded not to be treatment related.

Table 4 Incidence of lung proliferative lesions at the final sacrifice [a].

	Untreated	Vehicle	sph-SWCNH		CNB		MWCNT-7
			0.5 mg/rat	1 mg/rat	0.5 mg/rat	1 mg/rat	1 mg/rat
Number of rats examined	12	11	8	12	13	10	4[b]
Bronchioloalveolar Hyperplasia (BAH)	0	0	0	0	0	0	1
Bronchioloalveolar Adenoma (BAA)	0	0	0	1	0	0	0
Bronchioloalveolar Carcinoma (BAC)	0	0	0	0	0	0	1

Combined	0	0	0	1	0	0	2 *

Values indicate number of animals bearing the lesion

*P<0.05 vs vehicle, Fischer exact test (2 sided).

[a] Final sacrifice at 75 weeks for the MWCNT-7 group and 104 weeks for the sph-SWCNH and CNB groups.

[b]10 rats underwent terminal sacrifice at week 75. Six rats had mesothelial invasion into the lung tissue so the lungs of these rats could not be assessed for lung lesions. Therefore, only four rats could be assessed for lung lesions.

Table 5 Incidence of pleural mesothelioma in rats that for 55 weeks or longer [a].

	Untreated	Vehicle	sph-SWCNH		CNB		MWCNT-7 1 mg/rat
			0.5 mg/rat	1 mg/rat	0.5 mg/rat	1 mg/rat	
Number of rats examined	14	14	10	13	14	13	17
Visceral Mesothelioma	0	0	0	0	0	0	6
Parietal mesothelioma	0	0	0	0	0	0	13***
Combined [b]	0	0	0	0	0	0	13***

Values indicate number of animals bearing the lesions.

***P<0.001 vs vehicle respectively, Fischer exact test (2 sided).

[a] The first mesothelioma was found in the MWCNT-7 group at 55 weeks.

[b] 6 rats in tht MWCNT-7 group had both visceral and parietal mesotheliomas.

Table 6 Incidence of tumors in other organs at the final sacrifice [a]

	Untreated	Vehicle	sph-SWCNH		CNB		MWCNT-7 1 mg/rat
			0.5 mg/rat	1 mg/rat	0.5 mg/rat	1 mg/rat	
N. of rats examined [b]	14	14	10	13	14	13	17
Leydig cell tumor	7	10	9	9	11	7	1
Abdominal cavity mesothelioma	0	1	0	0	1	0	0
Leukemia	2	4	3	2	1	3	0
Subcutaneous fibroma	0	0	2	1	2	2	0
Thyroid tumor	1	0	0	0	0	0	0

Values indicate number of animals bearing the lesion

[a] final sacrifice at 75 weeks for the MWCNT-7 and 104week for the sph-SWCNH and CNB groups.

[b] Lived 55 weeks or longer: the first pleural mesothelioma was found in the MWCNT-7 group at week 55.

There is no significant difference in the treated groups compared to the vehicle (Fischer exact test, 2 sided).

Histopathological evaluation at the final sacrifice

Figure 9 shows the histopathological findings in the lung tissues of vehicle, sph-SWCNH, CNB, and MWCNT-7 treated rats at the final sacrifice. Table 7 shows the inflammatory and proliferative parameters in the lung and pleura at the final sacrifice. Compared to week 6, granuloma count decreased in all treated groups indicating the removal of fibers from the lung. However, the granuloma count was still significantly increased compared to the vehicle in all treated groups except for the 0.5 mg CNB treated group. In the 0.5 mg CNB group the granulation tissue count was higher, but not significantly higher, compared to the vehicle. For the MWCNT-7 treated rats, granuloma count was significantly higher compared to the 0.5 mg and 1 mg sph-SWCNH and CNB groups.

Immunohistochemical evaluation showed that the alveolar macrophage count in the rats administered 0.5 mg sph-SWCNH, 0.5 CNB, and 1 mg CNB was higher, but not significantly higher, compared to the vehicle. Rats administered 1 mg sph-SWCNH showed a mild but statistically significant increase in alveolar macrophage count compared to the vehicle group. In the MWCNT-7 treated rats, the macrophage count was significantly increased compared to the vehicle, sph-SWCNH, and CNB treated groups.

The PCNA indices of the lung and pleural tissues in the rats administered sph-SWCNH and CNB were not different from the vehicle. In contrast, the PCNA indices of both the lung and pleura in the rats administered MWCNT-7 were significantly increased compared to the vehicle, sph-SWCNH, and CNB treated groups.

Figure 9 Granuloma formation, CD68 positive macrophages, and alveolar epithelial cell proliferation at the final sacrifice.

(A) H.E staining. Lung granulomas in the alveolar space enclosing (b) sph-SWCNH, (c) CNB, (d) and MWCNT-7 are still present at 104 weeks in the sph-SWCNH and CNB treated rats and 75 weeks in the MWCNT-7 treated rats.

(B) CD68 (macrophage). The macrophage count is elevated in rats administered (b) sph-SWCNH, (c) CNB, (d) and MWCNT-7, with CD68 macrophage count significantly increased in the sph-SWCNH and MWCNT-7 treated rats.

(C) PCNA. The PCNA index is significantly elevated in the rats treated with In the MWCNT-7 (d), but not in the rats treated with sph-SWCNH (b) or CNB (c).

Table 7 Cell proliferation and inflammation related parameters in the lung tissue at the final sacrifice [a]

Lesions	Untreated	Vehicle	sph-SWCNH		CNB		MWCNT-7 1 mg/rat
			0.5 mg/rat	1 mg/rat	0.5 mg/rat	1 mg/rat	
Granuloma count /cm^2	0.6±0.4	8.3±5.2	23.7±8.5*	91.3±24.3**	16.5±7.2	54.4±13.2**	145.2±30.2$^{***,\#,\$\$}$
Macrophage count /cm^2	14.5±2.3	25.0±14.3	48.4±19.7	74.3±16.5**	23.4±9.4	46±14	376.5±20.2$^{***,\#\#,\$\$}$
Alveolar cell PCNA index %	4.8±1.2	7.2±1.6	8.8±1.8	9.3±3.1	5.3±1.1	9.8±1.7	33.6± 5.2$^{***,\#\#\#,\$\$\$}$
Pleural cell PCNA index %	0±0	0.8±0.4	1.1±0.2	1.4±0.4	0.6±0.2	1.2±0.5	21.6±4.1$^{***,\#\#\#,\$\$\$}$
Pulmonary Collagen deposition %	2.6±1.6	2.0±1.1	2.5±1.1	6.2±1.6 *	3.2±0.4	3.5±1.8	21.7±1.4$^{***,\#\#\#,\$\$\$}$
Subpleural Collagen deposition %	0.5±0.7	0.5±0.9	0.6±0.2	0.8±0.4	0.5±0.4	0.6±0.7	8.6±0.9$^{***,\#\#\#,\$\$\$}$

Values, mean ± S.D, No. of rats examined 5 rats/group

[a] Final sacrifice at 104 weeks for the sph-SWCNH and CNB groups and 75 weeks for the MWCNT-7 group

$^{*, **, ***}$ $p < 0.05, 0.01, 0.001$ vs Vehicle, respectively.

$^{\#, \#\#, \#\#\#}$ $p < 0.05, 0.01, 0.001$ vs sph-SWCNH 1 mg/rat, respectively.

$^{\$\$, \$\$\$}$ $p < 0.01, 0.001$ vs CNB 1 mg/rat, respectively.

Masson's trichrome staining of the lung and pleura in the vehicle, 1 mg sph-SWCNH, 1 mg CNB, and MWCNT-7 treated groups at the final sacrifice are shown in Figure 10, and pulmonary and sub-plural collagen deposition percentages in the vehicle, 0.5 and 1 mg sph-SWCNH, 0.5 and 1 mg CNB, and MWCNT-7 treated groups at the final sacrifice are shown in Table 7. The lung tissue of the 0.5 mg sph-SWCNH, 0.5 mg CNB, and 1 mg CNB treated rats did not show a difference in collagen deposition compared to the vehicle. In contrast, there was a moderate, but statistically significant, increase in the collagen deposition in the lungs of the 1 mg sph-SWCNH treated rats. Pulmonary collagen deposition was significantly higher in the 1 mg MWCNT-7 group compared to the vehicle. Fibrotic changes with increased deposition of collagen in the alveolar wall, parabronchial areas, and within the granulation tissues were observed in the MWCNT-7 group. Deposition of collagen in the sub-pleural space in the sph-SWCNH and CNB treated rats was not increased compared to the

vehicle group. In contrast, deposition of collagen fibers was markedly elevated in the sub-pleural space of rats treated with MWCNT-7.

Figure 10 Masson trichrome staining of the lung, visceral pleura, and parietal pleura at the final sacrifice. (A) Lung and visceral pleura. (B) Parietal pleura. Collagenous thickening of the alveolar wall, visceral pleura, and parietal pleura (blue in Masson's trichrome staining) is observed only in the MWCNT-7 treated group (d), but not in vehicle (a), sph-SWCNH (b) or CNB (c) groups (all are 1 mg/rat administered groups).

Discussion

In the present study, we investigated the pulmonary and pleural toxicity and carcinogenicity of spherical and fibrous aggregates of single walled carbon nanohorns (sph-SWCNHs and CNBs respectively) in the lungs of rats administered the test materials using TIPS. Rats were untreated or administered vehicle, 0.5 mg or 1.0 mg sph-SWCNH, 0.5 mg or 1.0 mg CNB, or 1.0 mg MWCNT-7 per rat. At 6 weeks, sph-SWCNH and CNB aggregates were phagocytosed by alveolar macrophages forming inflammatory granulomas, but these materials did not induce production of the pro-inflammatory cytokines or chemokines. The proliferative status of alveolar epithelial cells was not increased in the rats administered sph-SWCNH or CNB. At 2 years, all SWCNH aggregates found inside the lung were enclosed inside granulomas with no signs of persistent inflammation: only an extremely small amount of material was present in free macrophages. For sph-SWCNH treated rats, a single rat in the high dose group (1 mg/rat) developed a bronchioloalveolar adenoma, but development of a single tumor was not significant compared to the control group. For CNBs, no lung tumors developed in the treated rats. In the pleural mesothelium, no tumors developed in the sph-SWCNH or CNB groups. Also, no treatment related tumors were observed in other organs. In contrast to the sph-SWCNH and CNB groups, MWCNT-7 significantly increased the incidence of proliferative lung lesions and malignant pleural mesotheliomas (Table 4, 5, 6). The results of the lung and pleural carcinogenicity of MWCNT-7 in the current study were consistent with the results of previous studies (Numano et al. 2019 [17], Saleh et al. 2022 [21], and Hojo et a;. [15]). The present study is the first 2-year toxicity study to investigate the pulmonary toxicity, fibrogenesis, and carcinogenicity of sph-SWCNH and CNB after intratracheal administration into the rat lung. Our findings indicate that sph-SWCNH and CNB do not cause pulmonary toxicity or fibrogenesis and are not carcinogenic in the rat lung.

At six weeks, granulomas had developed in the lungs of rats treated with sph-SWCNH and CNB, and their count increased with increasing dose. In the MWCNT-7 treated group, the rats were administered the same dose as the high dose sph-SWCNH and CNB treated groups (1 mg/rat). MWCNT-7 fibers caused the development of more granulomas than sph-SWCNH and CNB. Also, sph-SWCNH and CNB increased the recruitment of CD68-positive alveolar macrophages into the lung compared to the vehicle, and the CD68-positive macrophage count were significantly increased in the lungs of MWCNT-7 treated rats compared to the sph-SWCNH and CNB treated rats. These results indicate that sph-SWCNHs and CNB fibers induced lung inflammation, but induction of inflammation was not chronic and was milder than that induced by MWCNT-7 fibers.

Production of proinflammatory cytokines and chemokines in the lung is an important pulmonary response to environmental stimuli. Gene expression analysis of inflammatory cytokines from the lungs of vehicle, sph-SWCNH, CNB, and MWCNT-7 treated rats at 6 weeks showed that Ccl2, Ccl3, and TNF-α were significantly upregulated in the MWCNT-7 treated rats, but not in the sph-SWCNH or CNB treated rats, compared to the vehicle (Figure 5). Gene expression of IL-1α, IL-1β, Cxcl-1, Cxcl-2, and Cxcl-3 was not changed by sph-SWCNH, CNB, or MWCNT-7 compared to the vehicle (Additional file 2). These results indicate that MWCNT-7 induced inflammation in the lung, but sph-SWCNH and CNB exhibited only transient, mild inflammatory potential in our study. These results are consistent with Lynch et al. (2007) who found that there were no statistically significant differences in the mRNA expression levels of approximately 46,000 genes extracted from the lungs of mice administered vehicle and 30 μg SWCNH by pharyngeal aspiration at 1- and 7- days post exposure [37].

MWCNT-7 also induced ROS production in alveolar epithelial cells and increased cell proliferative activity. In contrast, sph-SWCNH and CNB did not induce ROS production in alveolar epithelial cells or increase cell proliferative activity. These results are also in agreement with the results of Lynch et al. who found that the GSSG:GSH ratio (the ratio of oxidized to total glutathione) in lung homogenates, which is indicative of the overall pulmonary anti-oxidative balance, was not different in the SWCNH administered mice compared to the vehicle group [37]. These results indicate that the presence of SWCNH particles within pulmonary macrophages did not promote oxidative stress within the lung. Also, these results agree with the results of Horie et al. [38] who showed that the intratracheal instillation of SWCNH (referred to as CNH in their report) at 1 mg/rat induced transient oxidative stress in the rat lung that was resolved at 7 days after

instillation. Thus, our findings at week 6 (4 weeks after the final TIPS administration) are consistent with earlier short-term studies and indicate that sph-SWCNHs and CNBs did not affect lung cell proliferative activity or oxidative stress. Notably, these toxicity markers were elevated in the positive control group (MWCNT-7) and may predict carcinogenicity at 2 years.

At the final sacrifice, although, there was an increase in the granuloma count in the sph-SWCNH and CNB groups, the CD68-positive macrophage count did not increase compared to the vehicle group except in the high dose sph-SWCNH group. The granuloma count and CD68 positive macrophages were both increased in the MWCNT-7 treated group and were both significantly higher than in the sph-SWCNH and CNB groups. These findings indicate that although administration of sph-SWCNH and CNB into the lung resulted in recruitment of macrophages into the lung, neither persistent recruitment of macrophages into the lung nor persistent inflammation was induced. Notably while recruitment of macrophages into the lung was significantly higher in the 1.0 mg sph-SWCNH group compared to the vehicle group at 2 years, the sph-SWCNH group had significantly lower numbers of macrophages in the lung compared to the MWCNT-7 group. Thus, the disassembly of CNB aggregates and the presence of sph-SWCNH aggregates enclosed by granulomas at 2 years indicates that disassembly/sequestration of SWCNH aggregates in granulation tissue mitigates a biological reaction to these aggregates.

Thus, at both 6 weeks and 104 weeks, sph-SWCNHs and CNB fibers elicited a weaker biological response compared to the MWCNT-7 fibers. In the 0.5 mg sph-SWCNH group and the 0.5 and 1 mg CNB groups, no rats developed bronchioloalveolar hyperplasia, adenoma, or carcinoma (Table 4). In the high dose group (1 mg/rat) sph-SWCNH group, one rat developed bronchioloalveolar adenoma, however, development of a single tumor was not statistically different compared to the controls. Overall, the granuloma count, number of CD68 positive macrophages, alveolar epithelial and pleural mesothelial cell PCNA indices, and collagen deposition in the pulmonary and sub-pleural tissues in the sph-SWCNH and CNB groups were less than in the MWCNT-7 treated rats, and this was reflected in the lack of particle-induced development of lung tumors in the sph-SWCNH and CNB groups.

Chronic inflammation is a hallmark of cancer. A protracted inflammatory response is one mechanism that promotes DNA damage and mutations, proliferation of cells with mutated DNA, and their progression to carcinogenesis [39]. In the present study, administration of sph-SWCNH and CNB into the lung caused an increase in the number of CD-68 p[17]ositive macrophages in the alveolar space at 6 weeks (4 weeks after the

final administration), but recruitment of macrophages was not sustained in the lungs of the treated rats, and we found that 2 years after the administration of sph-SWCNH and CNB, biological reactions were almost absent (see Table 7), probably reflecting the ability of the lung to eliminate the sph-SWCNHs and CNB fibers or sequester carbon nanohorn aggregates in granulation tissue.

Another notable result in this study was the apparently low incidence of lung proliferative lesions in the MWCNT-7 treated rats: 1 rat developed bronchioloalveolar hyperplasia and 1 rat developed lung adenocarcinoma. In this group, 13 rats developed malignant mesotheliomas, which agrees with the cytotoxicity and pleural malignancy of MWCNT-7 administered into the rat lung using TIPS [17, 21]. The 4 rats which did not have mesothelial invasion into the lung were evaluated for the lung proliferative lesions and the incidence of lung tumor development in these 4 rats was significantly higher than the control groups. Notably, an incidence of 1 carcinoma in 4 rats agrees with the incidence of bronchioloalveolar carcinomas in a two-year inhalation study by Kasai et al. [16]. In the Kasai et al. study, 11 carcinomas developed in 50 male rats exposed to 2 mg/m^3 MWCNT-7 for 2 years [16]. A low incidence of lung tumor development accompanied by a high incidence of mesothelioma development was also observed in a previous study in which rats administered MWCNT-7 by TIPS died before the end of the study period due to mesothelioma [17]. Therefore, development of bronchioloalveolar tumors in rats treated with MWCNT-7 in the present study was similar to that reported previously. These results are also compatible with the study by Hojo et al. 2022 [15]They administered MWCNT-7 to rats using TIPS once every 4 weeks over the course of 2 years and 6 of 28 rats developed bronchioloalveolar carcinoma, 4 of 28 rats developed bronchioloalveolar adenoma, and 1 rat developed non-keratinizing epithelioma [15]. In addition, the MWCNT-7-treated rats had increased granuloma counts, increased numbers of CD68 macrophages, and an increased alveolar epithelial cell PCNA index at 6 weeks and at the final sacrifice. Thus, the carcinomas that developed in this group can be considered to be typical of bronchioloalveolar carcinomas induced by MWCNT-7.

Macrophages are the first line of defense not only against invading pathogens and microbes but also against environmental dust and crystals like silica, asbestos, and carbon nanotubes. Previous reports showed that macrophages could discriminate between the crystals through their receptors. Tsugita et al., reported that the class B scavenger receptor SR-B1 recognizes silica [40]. Omori et al., showed that Tim4 receptors recognize MWCNTs but not chrysotile asbestos, indicating that the Tim4 receptor is specific for MWCNTs rather than the fiber structure [41]. They reported that Tim4-Ig bound graphene, carbon nano test tubes, and

SWCNT and concluded that Tim4 directly binds CNTs through aromatic interactions. Notably they also reported that the SWCNTs used in their study did not stimulate macrophages to produce IL-1β. In the present study, we also found that administration of MWCNT-7 and sph-SWCNH and CNB did not cause increased expression of IL-1β in the lungs of rats at week 6. In contrast to these results, Naiki-Ito et al. reported that administration of SWCNT into the lungs of rats at a dose of 0.5 mg/rat did cause increased expression of IL-1β in the lungs of rats at week 4 (Naiki-Ito et al, unpublished observations). Importantly, the MWCNT used in the Omori et al. study markedly induced expression of IL-1β by mouse peritoneal macrophages when the macrophages were cultured for 3 hours with 10 μg/ml MWCNT. This indicates that the *in vitro* system used in the Omori study was responsive to CNTs and that exposure to CNTs could result in induction of IL-1β. Since sph-SWCNH and CNB and SWCNTs are composed of identical materials, single graphene tubules, the lack of IL-1β induction by SWCNTs in the Omori study agrees with the results of our present study. While the two studies had contrasting results with MWCNTs, the MWCNT used in the Omori study was not characterized and consequently cannot be compared directly with the effect of MWCNT-7 used in our study. However, both studies did demonstrate that MWCNTs induced the expression of inflammatory cytokines while SWCNT (Omori study) and sph-SWCNH and CNB (our present study) did not induce the expression of inflammatory cytokines. One possible explanation for the contrasting results of the Naiki-Ito et al. study that SWCNT administration into the lungs of rats did induce expression of inflammatory cytokines is that the effect of the SWCNTs was associated with material absorbed into the SWCNT agglomerate. A notable difference between SWCNT agglomerates and sph-SWCNH and CNB particles is that the sph-SWCNH and CNB particles are aggregates, not agglomerates, with little intra-particle space. Consequently, the loosely tangled SWCNT agglomerates will absorb much more material from the fluid lining the lung than sph-SWCNH and CNB particles. Therefore, the material with little or no material absorbed from the lung, i.e., the SWCNT used in the Omori study (cells exposed in-vitro) and the sph-SWCNH and CNB particles used in our present study, did not induce expression of inflammatory cytokines, while the SWCNT with substantial amount of absorbed material, i.e., the SWCNT used in the Naiki-Ito study, did induce expression of inflammatory cytokines. This also agrees with the lack of toxicity of thin flexible CNTs administered by intra-peritoneal injection [14]. This conjecture needs to be explored in future studies.

In conclusion, our 2-year observation of rats administered sph-SWCNH and CNB by TIPS revealed that neither sph-SWCNH nor CNB caused induction of inflammatory responses or cell proliferation in the lung or

pleura and no carcinogenic changes occurred. In addition, the lack of proliferative activity and lack of increased ROS levels in the alveolar epithelium at 6 weeks (4 weeks after the final TIPS administration) were associated with the lack of carcinogenicity, which may contribute to improved carcinogenicity detection in future studies.

Supplementary information

Additional File 1: Additional Table 1. Primers used for qt-PCR.

Additional File 2: Additional Table 2. Pro-inflammatory gene expression.

Additional File 3: Additional Table 3. ROS generation.

Additional File 4: Additional Table 4. Cause of death of the rats that died before week 55.

Additional File 5: Additional Figure 1. Kaplan Meier survival curve.

List of abbreviations

CNH	Carbon Nanohorn
SWCNH	Single Walled Carbon Nanohorn
sph-SWCNH	Spherical aggregate of Single Walled Carbon Nanohorns
CNB	Carbon NanoBrush
CNT	Carbon NanoTube
MWCNT	Multi-Walled Carbon NanoTube
TIPS	Intra-Tracheal Intra-Pulmonary Spraying
PCNA	Proliferating Cell Nuclear Antigen
ROS	Reactive Oxygen Species
SEM	Scanning Electron Microscopy
TEM	Transmission Electron Microscopy

Declarations

Ethics approval and consent to participate

The research protocol was approved by the Animal Care and Use Committee of Nagoya City University Medical School (approval number H27-P-5), and the research was conducted according to the Guidelines for the Care and Use of Laboratory Animals of Nagoya City University.

Consent for publication

Not applicable

Availability of data and materials

All data generated or analyzed during this study are included in this published article and its supplementary information files.

Competing interests

Ryota Yuge is employed by NEC. The remaining authors declare that they have no competing interests.

Funding

This study was supported by Health and Labour Sciences Research Grants from the Ministry of Health, Labour and Welfare, Japan (H27-kagaku-shitei-004, H30-kagaku-shitei-004, H25-kagaku-ippan-004, H28-kagaku-ippan-004, 19KD1001, 20KD1003, 22KD1003, 23KD1002); Research Grants from the Long-range Research Initiative (LRI） (2017–2019) of the Japan Chemical Industry Association; YOG Specified Nonprofit Corporation, Association for Promotion of Research on Risk Assessment (2018–2021); and the Cultural Affairs and Missions Sector, Ministry of higher education of the Arab republic of Egypt.

Authors' contributions

O.H.M.A. helped prepare and administer the materials used in the study, directed pathological examination, collected and prepared tissue samples, analyzed tissue samples, assisted in animal care and well-being, and drafted and wrote the manuscript. A.N.-I. contributed to the conception and design of the study, analyzed tissue samples, confirmed confirmed the pathological conclusions, and assisted in writing the manuscript. D.A. helped prepare and administer the materials used in the study, assisted in animal care and well-being, and assisted in writing the manuscript. D.M.S. contributed to the conception and design of the study and assisted

in pathological examination. W.A. helped prepare and administer the materials used in the study and assisted in animal care and well-being. H.T. (Hiroshi Takase) helped characterize the materials used in the study and performed SEM and TEM. S.T. contributed to the conception and design of the study, assisted in analysis of tissue samples, and confirmed the pathological conclusions. A.H. contributed to the conception and design of the study and confirmed the pathological analysis and analysis of tissue samples. R.Y., M.Y., and S.I. provided essential information on the stability of the SWCNH aggregates, helped purify the material for administration via TIPS, and assisted in writing the manuscript. HT (Hiroyuki Tsuda) contributed to the conception and design of the study and approved the final methodology, acquired funding for the study, assisted in pathological analysis and analysis of tissue samples, assisted in writing the manuscript, and gave final approval of the manuscript submitted for publication. All authors read and approved the final manuscript.

Acknowledgements

The would like to acknowledge the NEC Corporation (Kawasaki, Japan) for supplying the sph-SWCNH and CNB usied in this study.

References

1. Iijima S. Helical microtubules of graphitic carbon. nature. 1991;354 6348:56-8.

2. Gupta SS, Singh KP, Gupta S, Dusinska M, Rahman Q. Do Carbon Nanotubes and Asbestos Fibers Exhibit Common Toxicity Mechanisms? Nanomaterials (Basel). 2022;12 10; doi: 10.3390/nano12101708. https://www.ncbi.nlm.nih.gov/pubmed/35630938.

3. Muller J, Delos M, Panin N, Rabolli V, Huaux F, Lison D. Absence of carcinogenic response to multiwall carbon nanotubes in a 2-year bioassay in the peritoneal cavity of the rat. Toxicol Sci. 2009;110 2:442-8; doi: 10.1093/toxsci/kfp100. https://www.ncbi.nlm.nih.gov/pubmed/19429663.

4. Nagai H, Okazaki Y, Chew SH, Misawa N, Miyata Y, Shinohara H, et al. Intraperitoneal administration of tangled multiwalled carbon nanotubes of 15 nm in diameter does not induce mesothelial carcinogenesis in rats. Pathol Int. 2013;63 9:457-62; doi: 10.1111/pin.12093. https://www.ncbi.nlm.nih.gov/pubmed/24200157.

5. Nagai H, Okazaki Y, Chew SH, Misawa N, Yamashita Y, Akatsuka S, et al. Diameter and rigidity of multiwalled carbon nanotubes are critical factors in mesothelial injury and carcinogenesis. Proc Natl Acad Sci U S A. 2011;108 49:E1330-8; doi: 10.1073/pnas.1110013108. https://www.ncbi.nlm.nih.gov/pubmed/22084097.

6. Sakamoto Y, Nakae D, Fukumori N, Tayama K, Maekawa A, Imai K, et al. Induction of mesothelioma by a single intrascrotal administration of multi-wall carbon nanotube in intact male Fischer 344 rats. J Toxicol Sci. 2009;34 1:65-76; doi: 10.2131/jts.34.65. https://www.ncbi.nlm.nih.gov/pubmed/19182436.

7. Takagi A, Hirose A, Futakuchi M, Tsuda H, Kanno J. Dose-dependent mesothelioma induction by intraperitoneal administration of multi-wall carbon nanotubes in p53 heterozygous mice. Cancer Sci. 2012;103 8:1440-4; doi: 10.1111/j.1349-7006.2012.02318.x. https://www.ncbi.nlm.nih.gov/pubmed/22537085.

8. Takagi A, Hirose A, Nishimura T, Fukumori N, Ogata A, Ohashi N, et al. Induction of mesothelioma in p53+/- mouse by intraperitoneal application of multi-wall carbon nanotube. J Toxicol Sci. 2008;33 1:105-16; doi: 10.2131/jts.33.105. https://www.ncbi.nlm.nih.gov/pubmed/18303189.

9. Sargent LM, Porter DW, Staska LM, Hubbs AF, Lowry DT, Battelli L, et al. Promotion of lung adenocarcinoma following inhalation exposure to multi-walled carbon nanotubes. Part Fibre Toxicol. 2014;11:3; doi: 10.1186/1743-8977-11-3. https://www.ncbi.nlm.nih.gov/pubmed/24405760.

10. Grosse Y, Loomis D, Guyton KZ, Lauby-Secretan B, El Ghissassi F, Bouvard V, et al. Carcinogenicity of fluoro-edenite, silicon carbide fibres and whiskers, and carbon nanotubes. Lancet Oncol. 2014;15 13:1427-8; doi: 10.1016/S1470-2045(14)71109-X. https://www.ncbi.nlm.nih.gov/pubmed/25499275.

11. IARC. IARC Monographs on the Evaluation of Carcinogenic Risks to Humans. Some Nanomaterials and Some Fibres. Volume 111; IARC Publication: Lyon, France, 2017. Available online: https://publications.iarc.fr/Book-And-Report-Series/Iarc-Monographs-On-The-Identification-Of-Carcinogenic-Hazards-To-Humans/Some-Nanomaterials-And-Some-Fibres-2017 (accessed on 19 July 2025). 2017.

12. Donaldson K, Murphy F, Schinwald A, Duffin R, Poland CA. Identifying the pulmonary hazard of high aspect ratio nanoparticles to enable their safety-by-design. Nanomedicine (Lond). 2011;6 1:143-56; doi: 10.2217/nnm.10.139. https://www.ncbi.nlm.nih.gov/pubmed/21182425.

13. Donaldson K, Murphy FA, Duffin R, Poland CA. Asbestos, carbon nanotubes and the pleural mesothelium: a review of the hypothesis regarding the role of long fibre retention in the parietal pleura,

inflammation and mesothelioma. Part Fibre Toxicol. 2010;7:5; doi: 10.1186/1743-8977-7-5. https://www.ncbi.nlm.nih.gov/pubmed/20307263.

14. Ahmed OHM, Naiki-Ito A, Takahashi S, Alexander WT, Alexander DB, Tsuda H. A Review of the Carcinogenic Potential of Thick Rigid and Thin Flexible Multi-Walled Carbon Nanotubes in the Lung. Nanomaterials (Basel). 2025;15 3; doi: 10.3390/nano15030168. https://www.ncbi.nlm.nih.gov/pubmed/39940144.

15. Hojo M, Maeno A, Sakamoto Y, Ohnuki A, Tada Y, Yamamoto Y, et al. Two-year intermittent exposure of a multiwalled carbon nanotube by intratracheal instillation induces lung tumors and pleural mesotheliomas in F344 rats. Part Fibre Toxicol. 2022;19 1:38; doi: 10.1186/s12989-022-00478-7. https://www.ncbi.nlm.nih.gov/pubmed/35590372.

16. Kasai T, Umeda Y, Ohnishi M, Mine T, Kondo H, Takeuchi T, et al. Lung carcinogenicity of inhaled multi-walled carbon nanotube in rats. Part Fibre Toxicol. 2016;13 1:53; doi: 10.1186/s12989-016-0164-2. https://www.ncbi.nlm.nih.gov/pubmed/27737701.

17. Numano T, Higuchi H, Alexander DB, Alexander WT, Abdelgied M, El-Gazzar AM, et al. MWCNT-7 administered to the lung by intratracheal instillation induces development of pleural mesothelioma in F344 rats. Cancer Sci. 2019;110 8:2485-92; doi: 10.1111/cas.14121. https://www.ncbi.nlm.nih.gov/pubmed/31265162.

18. Suzui M, Futakuchi M, Fukamachi K, Numano T, Abdelgied M, Takahashi S, et al. Multiwalled carbon nanotubes intratracheally instilled into the rat lung induce development of pleural malignant mesothelioma and lung tumors. Cancer Sci. 2016;107 7:924-35; doi: 10.1111/cas.12954. https://www.ncbi.nlm.nih.gov/pubmed/27098557.

19. Ahmed OHM, Saleh DM, Alexander WT, Takase H, Taquahashi Y, Hojo M, et al. Comparative Carcinogenicity of Double-Walled Carbon Nanotubes of Different Lengths Administered by Intratracheal Installation into Rat Lungs. Nanomaterials (Basel). 2025;15 18; doi: 10.3390/nano15181402. https://www.ncbi.nlm.nih.gov/pubmed/41003038.

20. Saleh DM, Alexander WT, Numano T, Ahmed OHM, Gunasekaran S, Alexander DB, et al. Comparative carcinogenicity study of a thick, straight-type and a thin, tangled-type multi-walled carbon nanotube administered by intra-tracheal instillation in the rat. Part Fibre Toxicol. 2020;17 1:48; doi: 10.1186/s12989-020-00382-y. https://www.ncbi.nlm.nih.gov/pubmed/33054855.

21. Saleh DM, Luo S, Ahmed OHM, Alexander DB, Alexander WT, Gunasekaran S, et al. Assessment of the toxicity and carcinogenicity of double-walled carbon nanotubes in the rat lung after intratracheal instillation: a two-year study. Part Fibre Toxicol. 2022;19 1:30; doi: 10.1186/s12989-022-00469-8. https://www.ncbi.nlm.nih.gov/pubmed/35449069.

22. Bethune DS, Kiang CH, De Vries M, Gorman G, Savoy R, Vazquez J, et al. Cobalt-catalysed growth of carbon nanotubes with single-atomic-layer walls. Nature. 1993;363 6430:605-7.

23. Iijima S, Ichihashi T. Single-shell carbon nanotubes of 1-nm diameter. nature. 1993;363 6430:603-5.

24. Honda K, Naya M, Takehara H, Kataura H, Fujita K, Ema M. A 104-week pulmonary toxicity assessment of long and short single-wall carbon nanotubes after a single intratracheal instillation in rats. Inhal Toxicol. 2017;29 11:471-82; doi: 10.1080/08958378.2017.1394930. https://www.ncbi.nlm.nih.gov/pubmed/29110549.

25. Iijima S, Yudasaka M, Yamada R, Bandow S, Suenaga K, Kokai F, et al. Nano-aggregates of single-walled graphitic carbon nano-horns. Chemical physics letters. 1999;309 3-4:165-70.

26. Harris PJ. New perspectives on the structure of graphitic carbons. Critical reviews in solid state and materials sciences. 2005;30 4:235-53.

27. Harris PJ, Tsang SC, Claridge JB, Green ML. High-resolution electron microscopy studies of a microporous carbon produced by arc-evaporation. Journal of the Chemical Society, Faraday Transactions. 1994;90 18:2799-802.

28. Iijima S. Carbon nanotubes: past, present, and future. Physica B: Condensed Matter. 2002;323 1-4:1-5.

29. Zhang M, Yamaguchi T, Iijima S, Yudasaka M. Individual single-wall carbon nanohorns separated from aggregates. The Journal of Physical Chemistry C. 2009;113 26:11184-6.

30. Yuge R, Nihey F, Toyama K, Yudasaka M. Preparation and Characterization of Newly Discovered Fibrous Aggregates of Single-Walled Carbon Nanohorns. Adv Mater. 2016;28 33:7174-7; doi: 10.1002/adma.201602022. https://www.ncbi.nlm.nih.gov/pubmed/27226221.

31. Yuge R, Nihey F, Toyama K, Yudasaka M. Carbon nanotubes forming cores of fibrous aggregates of carbon nanohorns. Carbon. 2017;122:665-8.

32. Zhang M, Yudasaka M. Carbon nanohorns and their high potential in biological applications. Carbon Nanoparticles and Nanostructures: Springer; 2016. p. 77-107.

33. Kosaka M, Yuge R. Resistivity of individual fibrous aggregates of carbon nanohorns. Carbon Trends. 2025:100531.

34. Streit JK, Bachilo SM, Naumov AV, Khripin C, Zheng M, Weisman RB. Measuring single-walled carbon nanotube length distributions from diffusional trajectories. ACS Nano. 2012;6 9:8424-31; doi: 10.1021/nn3032744. https://www.ncbi.nlm.nih.gov/pubmed/22924324.

35. Miyawaki J, Yudasaka M, Azami T, Kubo Y, Iijima S. Toxicity of single-walled carbon nanohorns. ACS Nano. 2008;2 2:213-26; doi: 10.1021/nn700185t. https://www.ncbi.nlm.nih.gov/pubmed/19206621.

36. Kohyama N, Suzuki Y. Analysis of asbestos fibers in lung parenchyma, pleural plaques, and mesothelioma tissues of North American insulation workers. Annals of the New York Academy of Sciences. 1991;643:27-52.

37. Lynch RM, Voy BH, Glass DF, Mahurin SM, Zhao B, Hu H, et al. Assessing the pulmonary toxicity of single-walled carbon nanohorns. Nanotoxicology. 2007;1 2:157-66.

38. Horie M, Komaba LK, Fukui H, Kato H, Endoh S, Nakamura A, et al. Evaluation of the biological influence of a stable carbon nanohorn dispersion. Carbon. 2013;54:155-67.

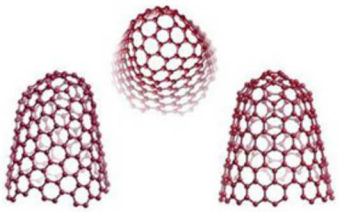
39. Borm PJ, Lison D, Driscoll K, Duffin R, Harkema J, Weber K, et al. Inflammation as a key outcome pathway in particle induced effects in the lung. Frontiers in public health. 2022;10:869041.

40. Tsugita M, Morimoto N, Tashiro M, Kinoshita K, Nakayama M: SR-B1 is a silica receptor that mediates canonical Inflammasome activation. Cell Rep. 2017; 18 (5): 1298–311. Epub 2017/02/02. doi: 10.1016/j. celrep. 2017.01. 004. PubMed PMID: 28147282.

41. Omori S, Tsugita M, Hoshikawa Y, Morita M, Ito F, Yamaguchi S-I, et al. Tim4 recognizes carbon nanotubes and mediates phagocytosis leading to granuloma formation. Cell reports. 2021;34 6.

SWCNH:
Single walled carbon nanohorns are composed of single graphene cylinders which are closed at one end

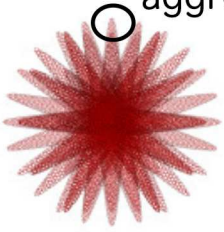
(a)



Spherical aggregate

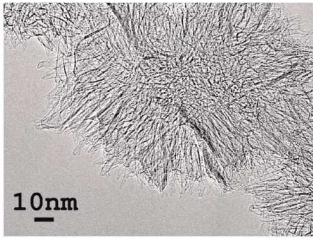
sph-SWCNH:
Spherical aggregate of single walled carbon nanohorns

(b)



TEM

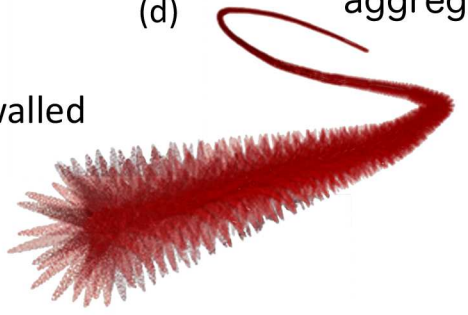
(c)



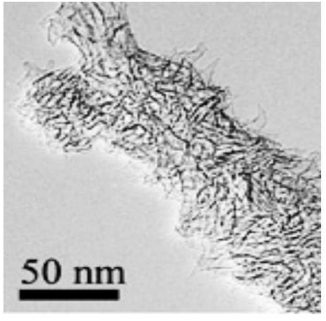
CNB:
Test tube brush like aggregate of single walled carbon nanohorns

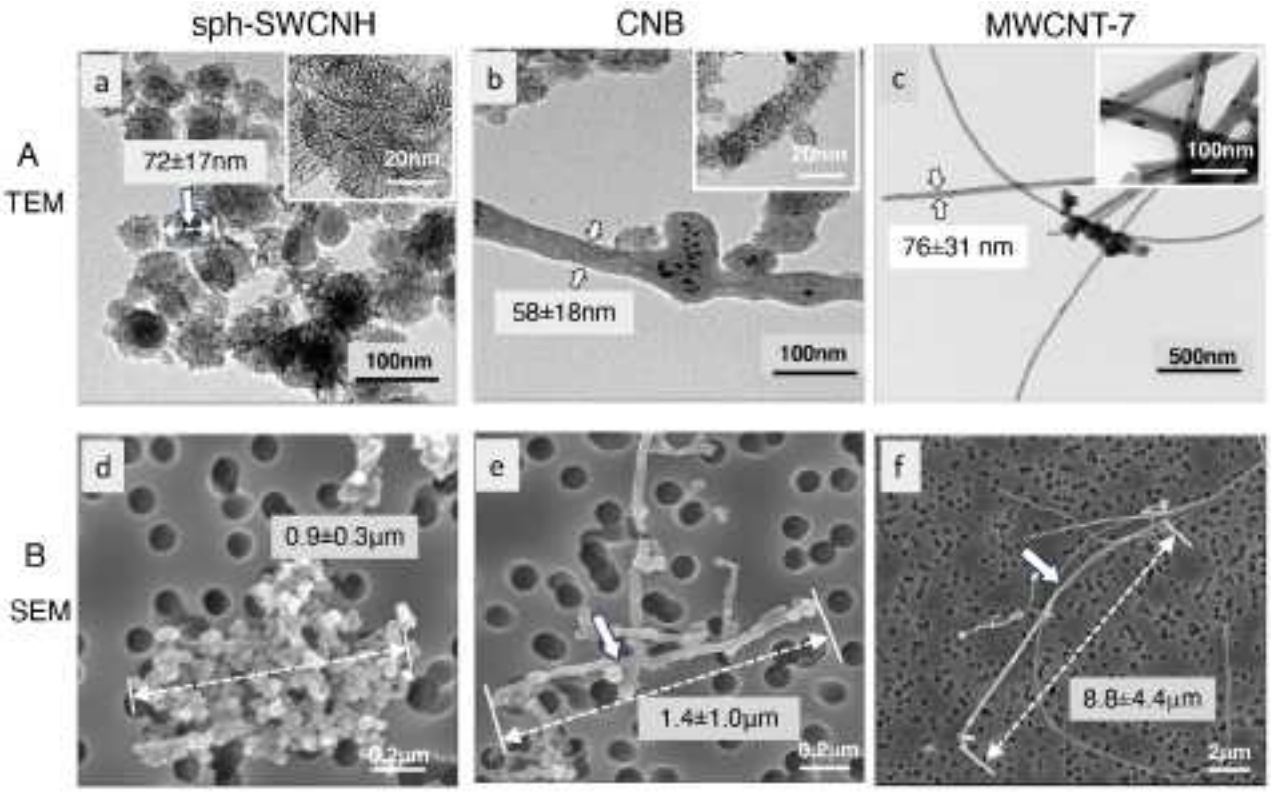
(d)

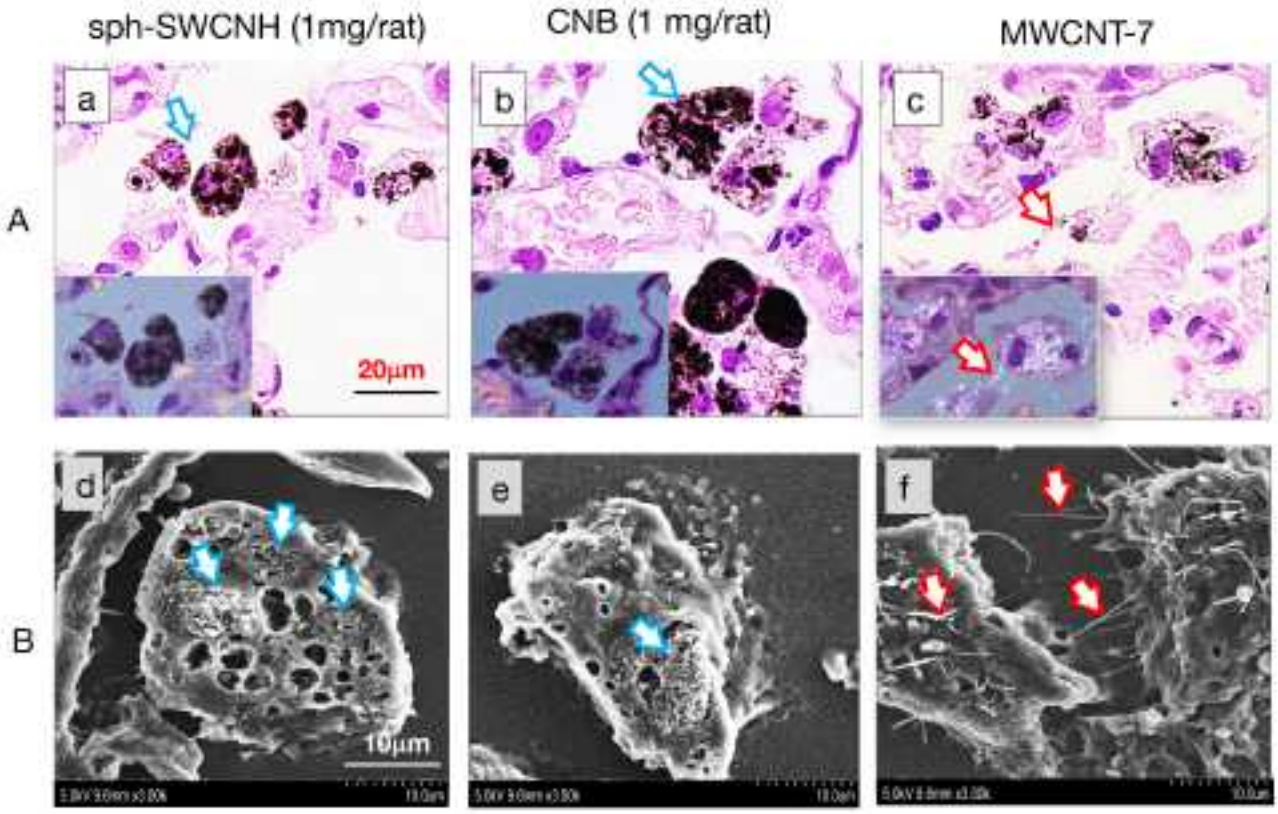
Brush like aggregate



(e)




sph-SWCNH
CNB
MWCNT-7
A
TEM
a
72±17nm
20nm
100nm
b
20nm
58±18nm
100nm
c
100nm
76±31 nm
500nm
B
SEM
d
0.9±0.3μm
0.2μm
e
1.4±1.0μm
0.2μm
f
8.8±4.4μm
2μm


sph-SWCNH (1mg/rat)
CNB (1 mg/rat)
MWCNT-7
A
a
b
c
20μm
B
d
e
f
10μm

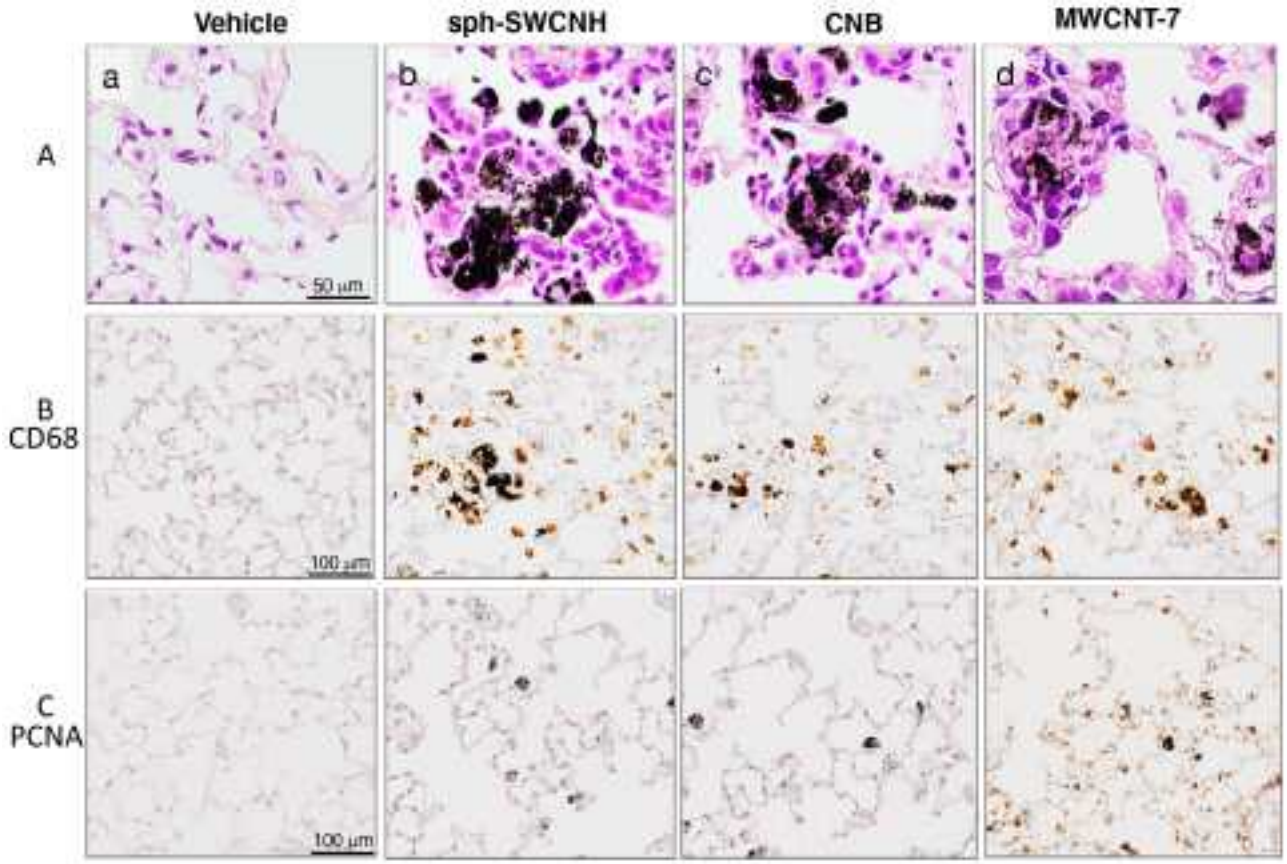
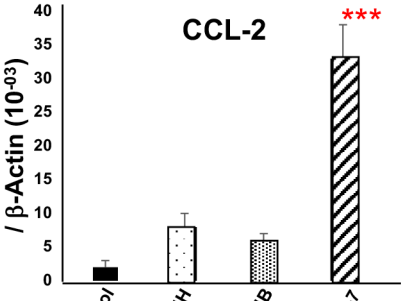
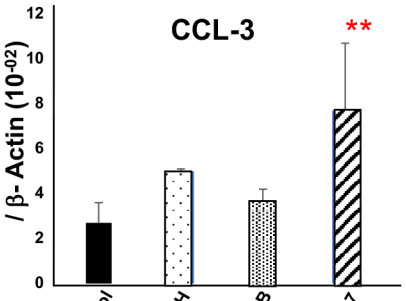
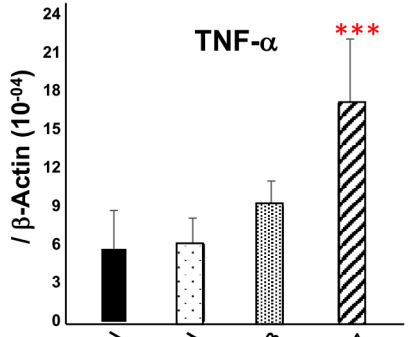

Vehicle
sph-SWCNH
CNB
MWCNT-7
a
b
c
d
A
50 µm
B
CD68
100 µm
C
PCNA
100 µm

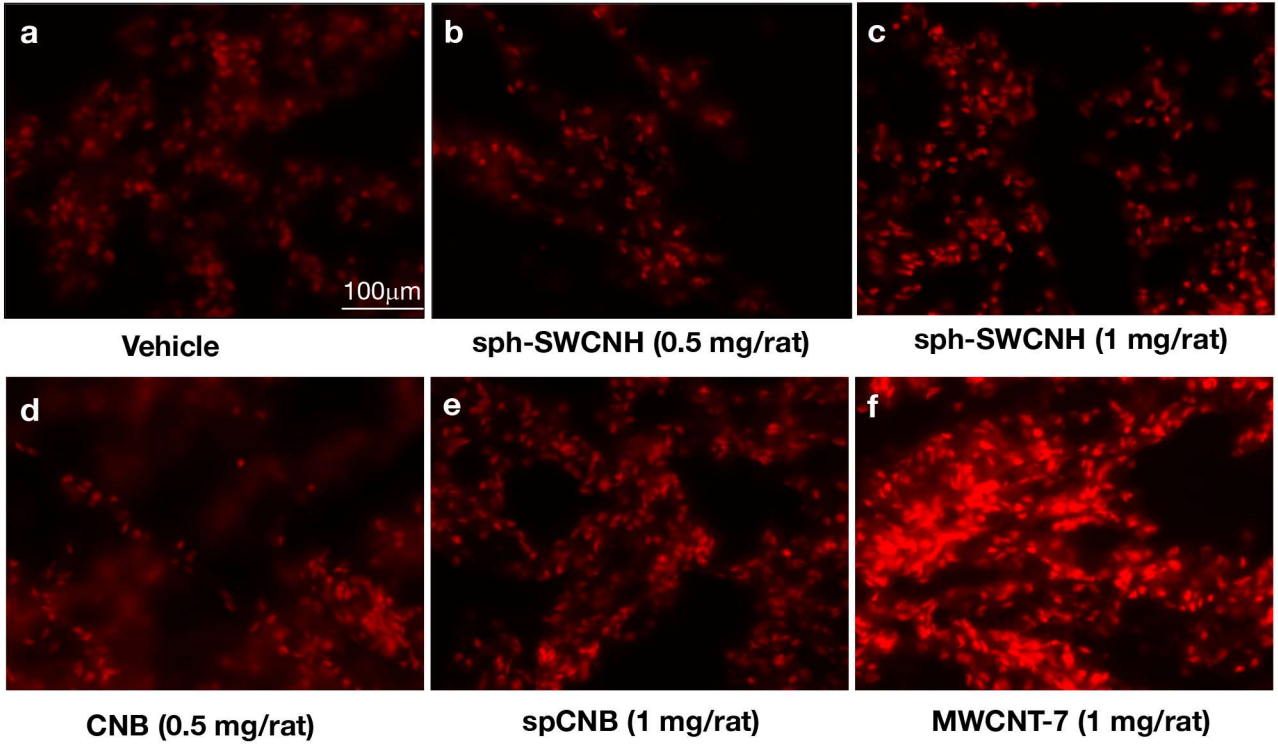
fig 5


CCL-2
***
/ β-Actin (10-03)
40
35
30
25
20
15
10
5
0
Control
sph-SWCNH
CNB
MWCNT-7


CCL-3
**
/ β- Actin (10-02)
12
10
8
6
4
2
0
Control
sph-SWCNH
CNB
MWCNT-7


TNF-α
***
/ β-Actin (10-04)
24
21
18
15
12
9
6
3
0
Control
sph-SWCNH
CNB
MWCNT-7

A fig 6


a
100μm
Vehicle
b
sph-SWCNH (0.5 mg/rat)
c
sph-SWCNH (1 mg/rat)
d
CNB (0.5 mg/rat)
e
spCNB (1 mg/rat)
f
MWCNT-7 (1 mg/rat)

B

Fig 6

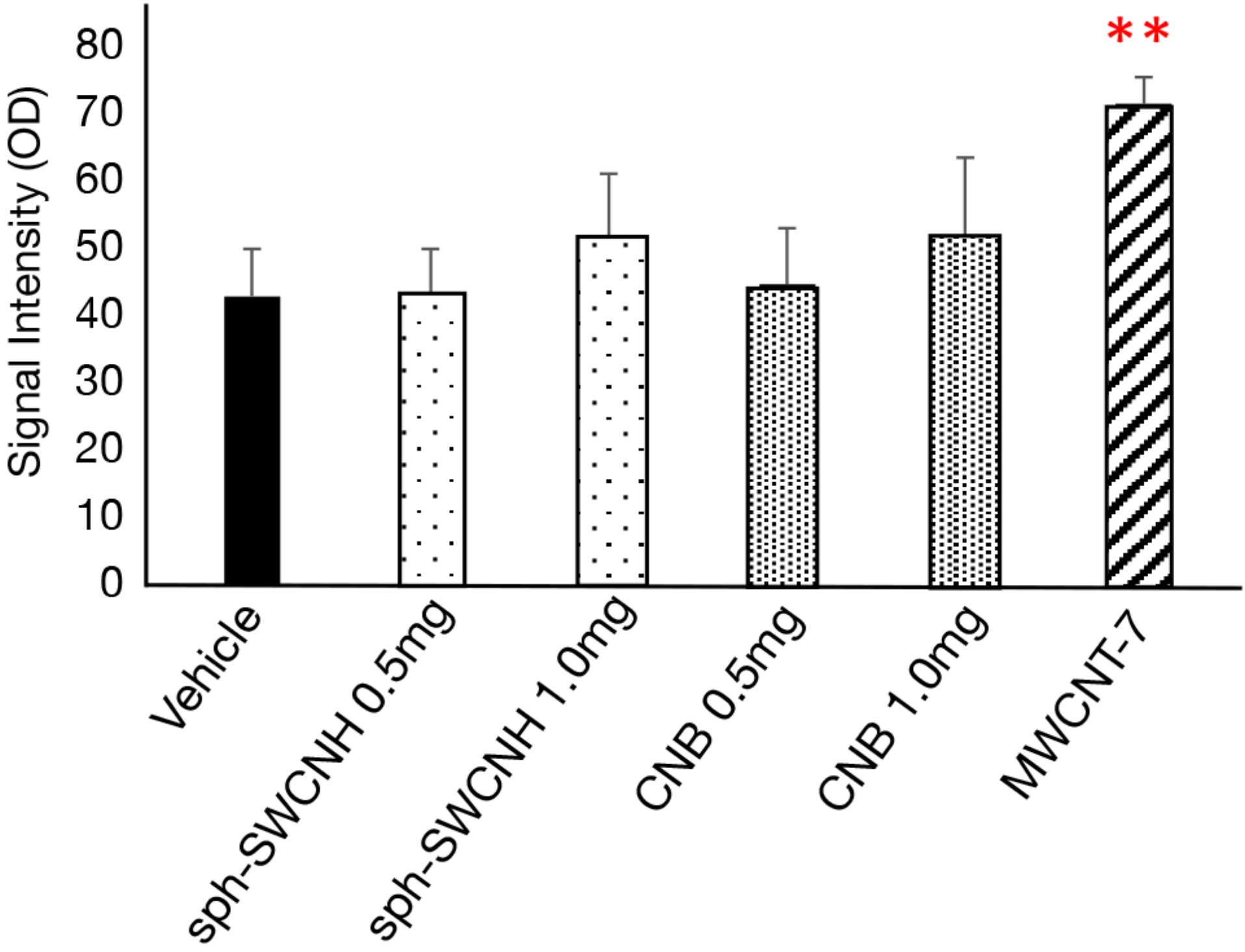

Signal Intensity (OD)
80
70
60
50
40
30
20
10
0
**
Vehicle
sph-SWCNH 0.5mg
sph-SWCNH 1.0mg
CNB 0.5mg
CNB 1.0mg
MWCNT-7

fig 7

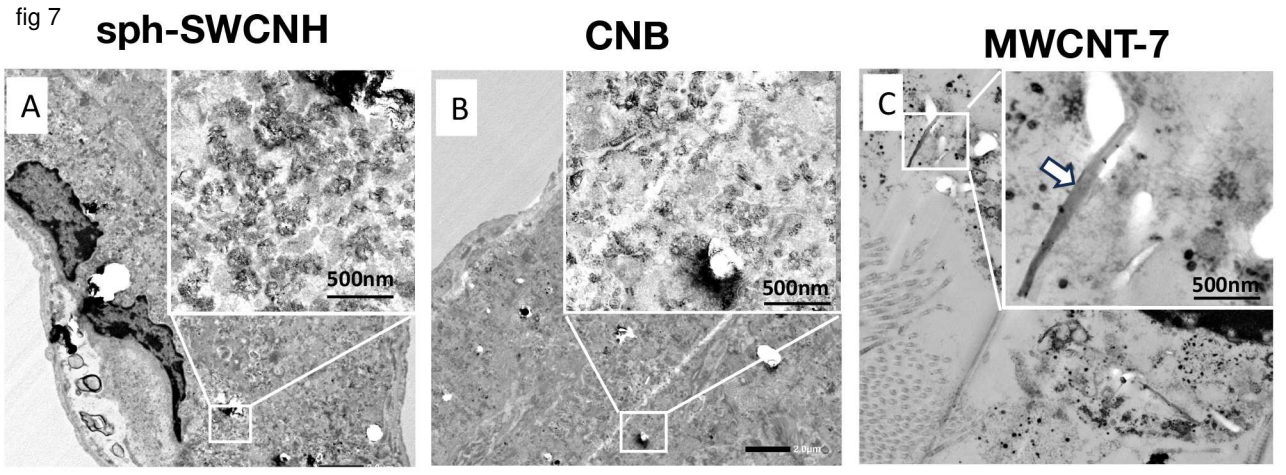
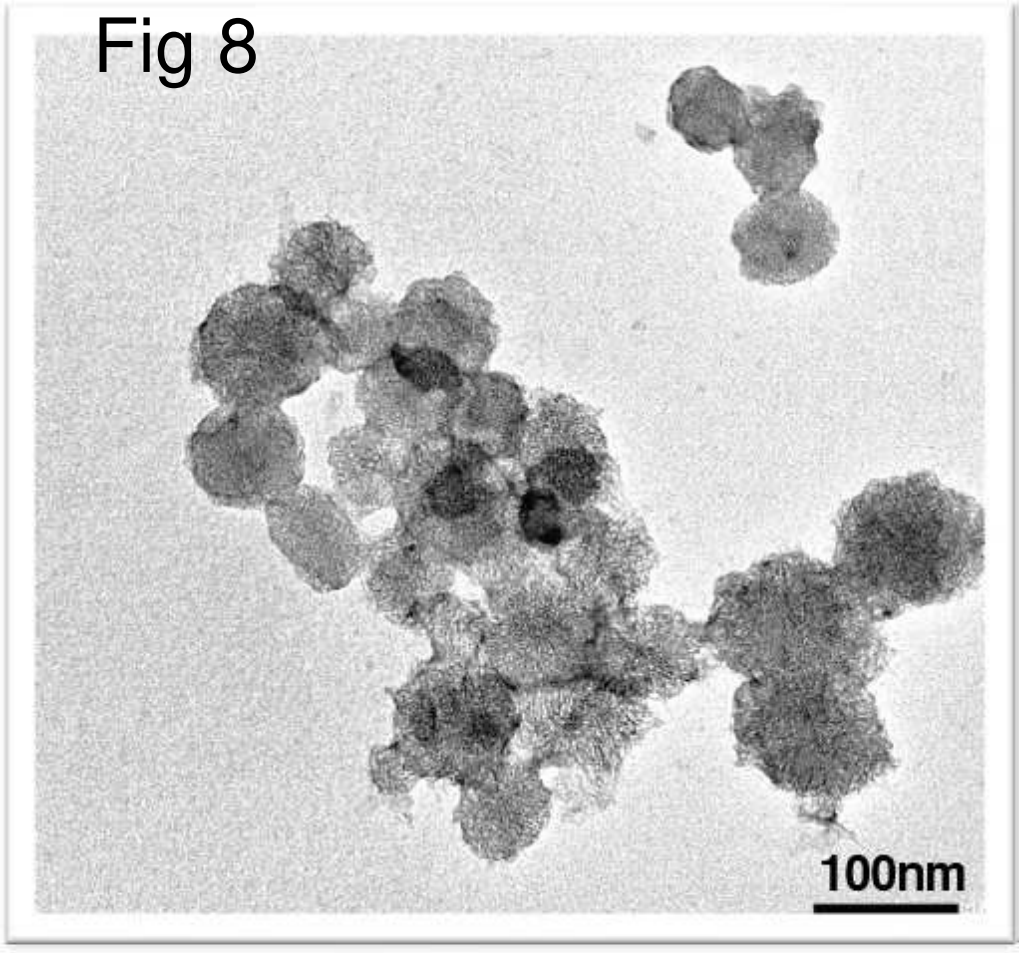
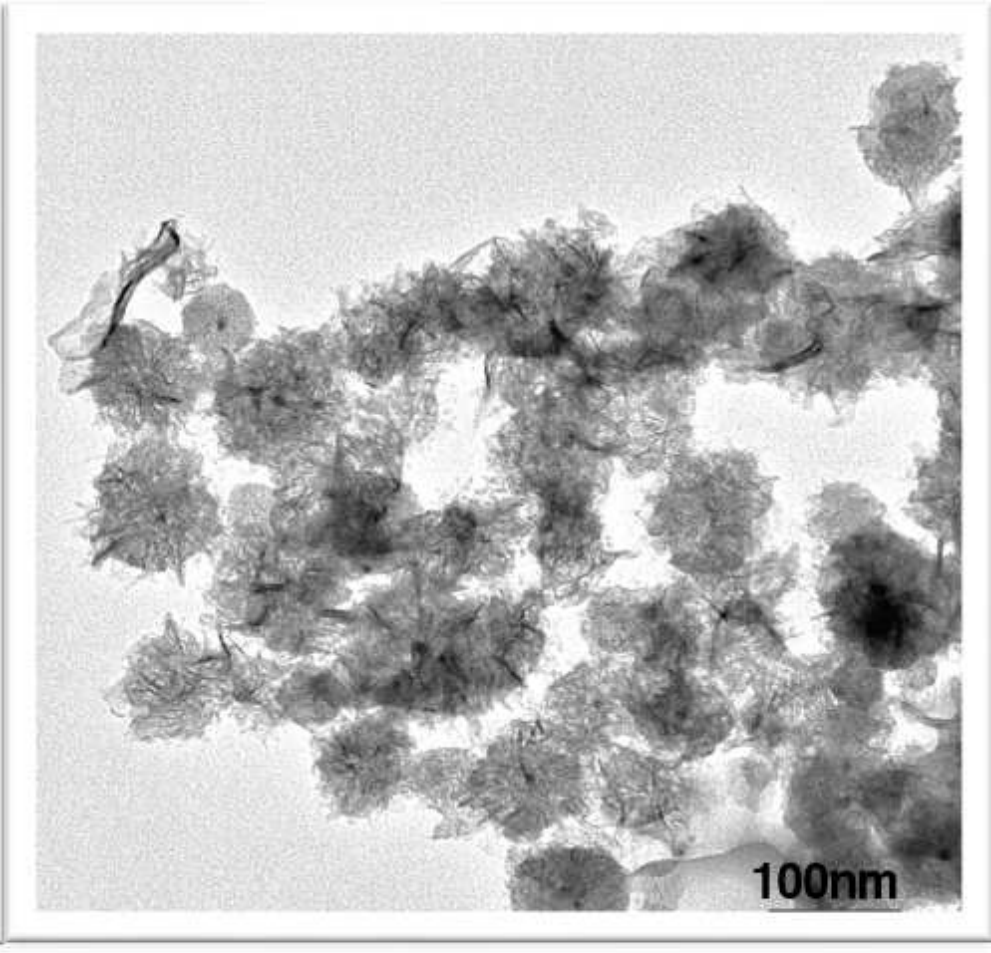


Fig 8





sph-SWCNH

CNB

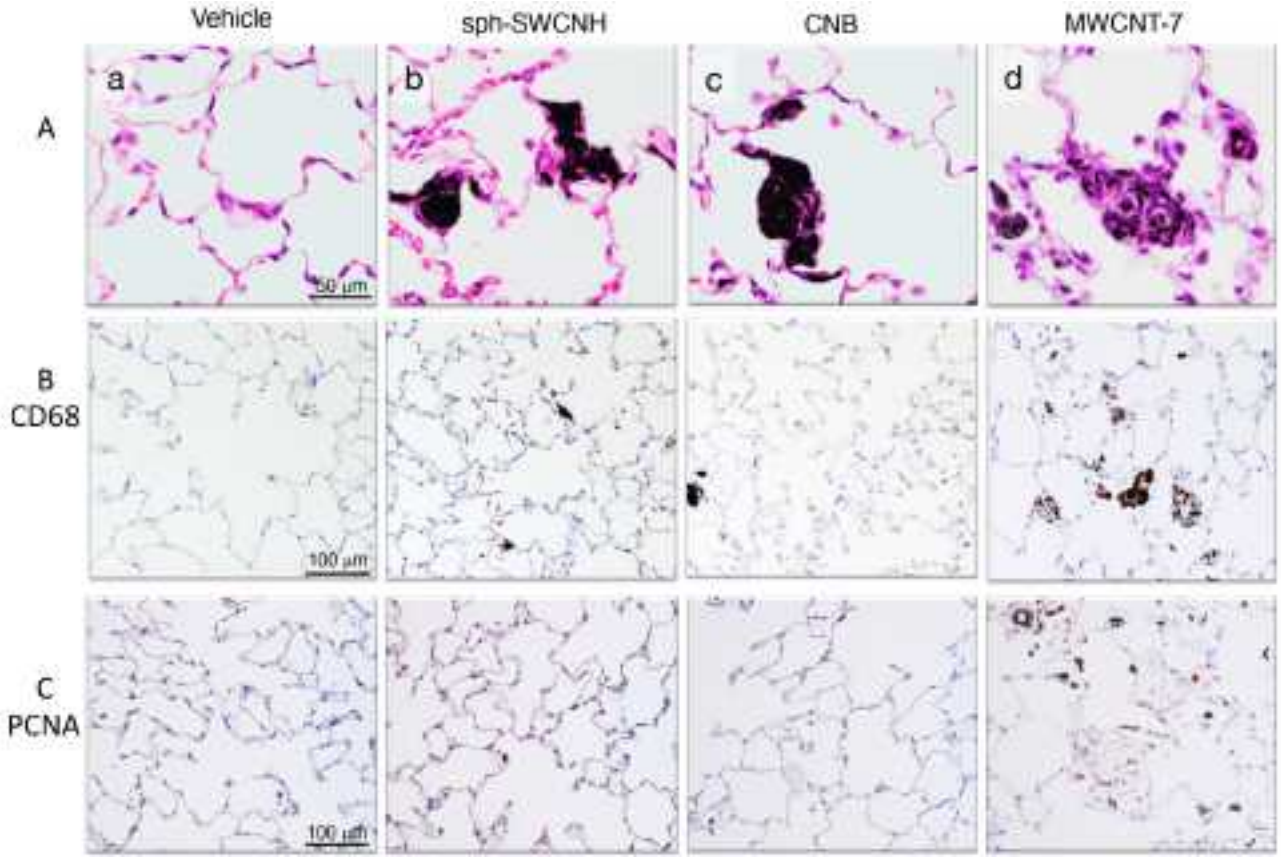
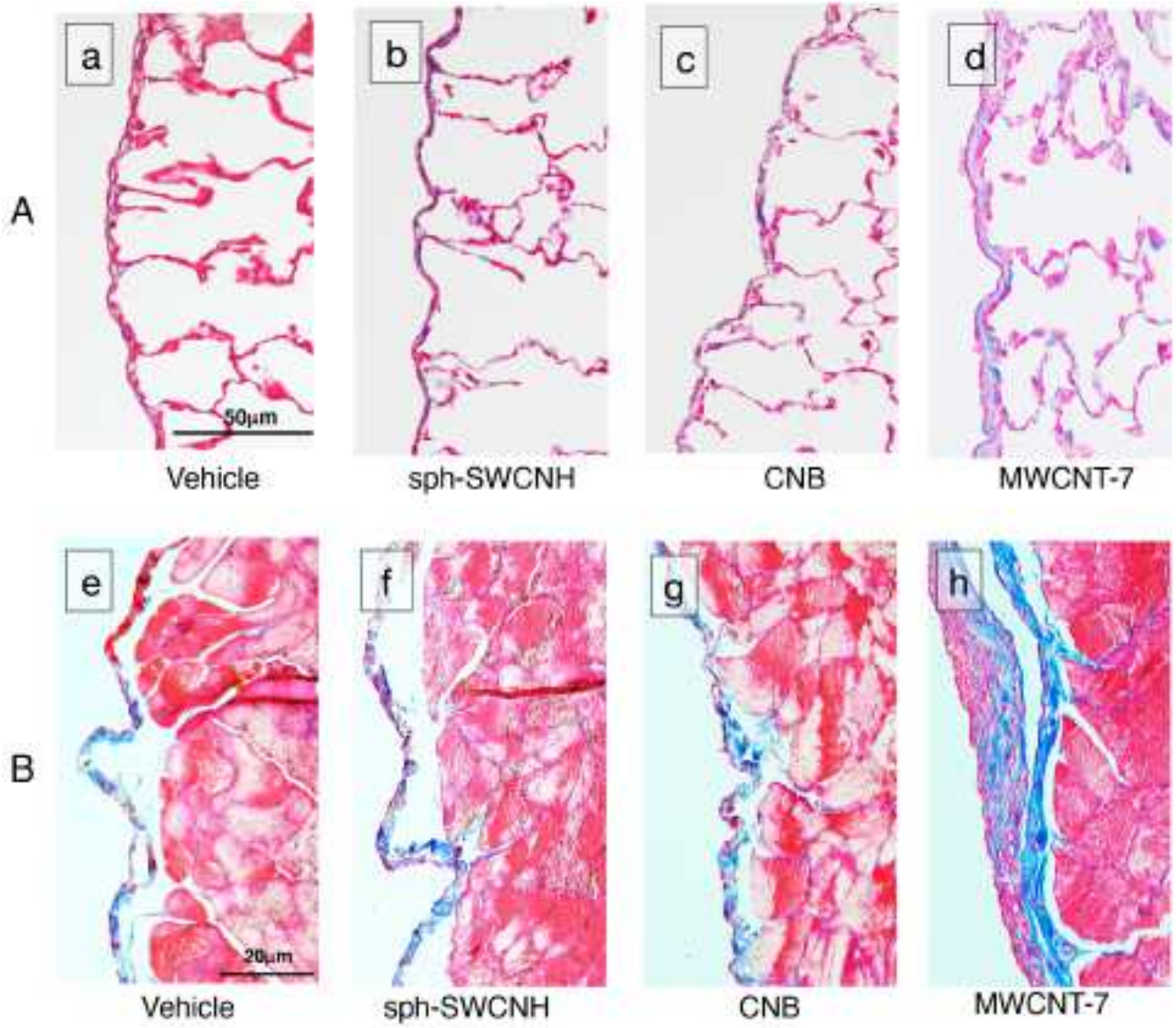

Vehicle
sph-SWCNH
CNB
MWCNT-7
A
a
b
c
d
50 μm
B
CD68
100 μm
C
PCNA
100 μm

Fig 10


A
a
50μm
Vehicle
b
sph-SWCNH
c
CNB
d
MWCNT-7
B
e
20μm
Vehicle
f
sph-SWCNH
g
CNB
h
MWCNT-7

Supplementary Files

This is a list of supplementary files associated with this preprint. Click to download.

- AdditionalFile1.docx
- AdditionalFile2.docx
- AdditionalFile3.tif
- AdditionalFile4.tif
- AdditionalFile5.tif